Journal of the Neurological Sciences 300 (2011) 67–73

Contents lists available at ScienceDirect

Journal of the Neurological Sciences

journal homepage: www.elsevier.com/locate/jns

Higher activity of peripheral blood angiotensin-converting enzyme is associated with later-onset of Alzheimer's disease

Hiroyasu Akatsu [a,*], Norihiro Ogawa [a], Takeshi Kanesaka [a], Akira Hori [a], Takayuki Yamamoto [a], Noriyuki Matsukawa [b], Makoto Michikawa [c]

[a] Choju Medical Institute, Fukushimura Hospital, Toyohashi, Aichi 441-8124, Japan
[b] Department of Neurology and Neuroscience, Nagoya City University Graduate School of Medical Sciences, Nagoya, Aichi 467-8601, Japan
[c] Department of Alzheimer's Disease Research, National Institute for Longevity Sciences, National Center for Geriatrics and Gerontology, Obu, Aichi 474-8522, Japan

ARTICLE INFO

Article history:
Received 10 March 2010
Received in revised form 22 September 2010
Accepted 24 September 2010
Available online 1 November 2010

Keywords:
Angiotensin-converting enzyme
Amyloid-β
Alzheimer's disease

ABSTRACT

According to the amyloid theory, the balance between amyloid-β (Aβ) production and degradation is key to the development of Alzheimer's disease (AD). Several enzymes including angiotensin-converting enzyme (ACE) have been reported as candidate enzymes involved in Aβ degradation. We previously identified the relationship between ACE activity and AD. We present a comparison between AD and non-AD patients in the inpatient care unit of a geriatric hospital and have included the onset age and age at sampling in the comparison. We performed a colorimetric assay to determine ACE activity and a sandwich enzyme-linked immunosorbent assay (ELISA) to quantify blood plasma Aβ 1–40 and 1–42 levels. Our 676 subjects, none of whom had received ACE inhibitor medication, included 147 AD patients. Clinical diagnoses were carried out to separate subjects into the AD and non-AD groups on the basis of the criteria of the International Classification of Diseases (ICD-10) and the Consortium to Establish a Registry for AD (CERAD).
We found that the later the onset of AD, the higher the ACE activity, but there was no correlation between ACE activity and the Aβ level in peripheral blood. In this report, we suggest that peripheral ACE activity may affect the age at AD onset.

1. Introduction

An increased amyloid-β (Aβ) protein level in the brain is considered to be a cause of Alzheimer's disease (AD), particularly when the formation of Aβ oligomer is synaptotoxic [1]. A high oligomer level with a poor turnover is currently considered to have a strong effect on the onset and progression of AD. The therapeutical goal, therefore, is to decrease the level of Aβ oligomers.

In studies on Aβ production, analysis of early-onset familial AD (FAD) has led to considerable medical breakthroughs. Mutations in the amyloid precursor protein (APP), presenilin 1 (PS1), PS2 genes were found in the majority of pedigreed cases of early-onset FAD [2,3]; these mutations were reported to lead to abnormal Aβ cleavage and deposition [4]. In addition, Aβ degradation has been associated with several enzymes including Aβ-degrading peptidase [5,6], neprilysin (NEP) [7], insulin-degrading enzyme (IDE) [8,9], cathepsin B [10], and angiotensin-converting enzyme (ACE) [11–13].

ACE is an endopeptidase that converts angiotensin (AGT.) I to AGT II, an activity that is strongly associated with hypertension and vascular dysfunction. Moreover, ACE inhibitors (ACE-Is) are recommended as the first-choice depressor drugs by the American College of Cardiology/American Heart Association Task Force on Practice Guidelines.

We found that mouse and human brain homogenates contain an enzyme that converts Aβ1–42 to Aβ1–40 and that the major portion of this converting activity is mediated by ACE [13]. Based in these findings, we suggest ACE activity may be critically important in the stage that precedes AD onset.

The ACE gene contains an insertion/deletion (I/D) polymorphism in intron 16, which has an effect on ACE activity and the level of the enzyme in plasma [14–19]. In addition, genetic variation at the ACE gene locus has been associated with ethnicity and shown to affect the vascular response to bradykinin [20]. Several groups have analyzed the relationship between this ACE gene polymorphism and AD, and the results showed that I allele carriers who might have a low ACE activity could be at risk of developing AD [21–26]. Using animal models, several investigators found that ACE activity decreases with age [27–30], but the situation in humans remains unclear. The greatest risk of sporadic AD is age-related. Therefore, it is essential to clarify the relationships of plasma ACE activity and AD onset with age. In addition, the relationships of ACE activity with Aβ1–42 and Aβ1–40 levels in plasma have also not been clarified, although we have shown that ACE converts Aβ1–42 to 1–40 and degrades Aβ [13].

* Corresponding author. Choju Medical Institute, Fukushimura Hospital, 19-14 Azayamanaka, Noyori, Toyohashi, Aichi 441-8124, Japan. Tel.: +81 532 46 7511; fax: +81 532 46 8940.
E-mail address: akatu@chojuken.net (H. Akatsu).

0022-510X/$ – see front matter © 2010 Elsevier B.V. All rights reserved.
doi:10.1016/j.jns.2010.09.030

To clarify these points, we quantified Aβ1–42 and Aβ1–40, and determined ACE activity using samples from both AD and non-AD groups. We then analyzed the fluctuation in ACE activity relative to the levels of Aβ1–42 and Aβ1–40 and investigated their correlations with age at onset and the type of blood sample used for analysis.

Cerebrospinal fluid (CSF) is a useful source of the laboratory AD biomarkers Aβ and phosphorylated tau, whereas peripheral blood has been proven less satisfactory. However, the information obtained here on AD-related ACE activity indicates that peripheral blood could be extremely useful in future studies.

2. Materials and methods

2.1. Patients

The 676 subjects of this study, none of whom had received ACE-I medication, included 147 AD patients who were admitted to Fukushimura Hospital or its nursing home, their families, and staff volunteers. We obtained the informed consent of patients and volunteers to use their samples in biochemical, molecular biological, and genomic research. Written informed consent was obtained from each subject in accordance with the protocol approved as application number 180 by the Ethics Committee of Fukushimura Hospital on October 6th, 2005.

2.2. Clinical diagnosis and subgrouping

Clinical information, including illness history, medication, and present illness, was obtained from the clinical records and by interview of the patients themselves or their families. We also carried out computed tomography (CT) of the brains of all the in-patients. All the subjects were classified into either the AD or non-AD group.

We used the criteria of ICD-10 and CERAD [26] for the clinical diagnostics of AD. We further divided the non-AD group into three subgroups: 1) the completely normal group (CN), physiologically and psychologically normal without medication; 2) the normal brain group (NB), having few physiological problems, such as hypertension, controlled with medication and no psychological problems; and 3) the abnormal brain group (AbB), with disorders of vascular, infectious, neurodegenerative, or psychosomatic nature. The AbB group was subdivided into three subgroups; the group with vascular problems (VP), the group with neurodegenerative disease (ND), and the group with other brain disorders (Oth). The VP group included patients with cerebral infarction (CI), cerebral hemorrhage (CH), subarachnoid hemorrhage (SAH), subdural hemorrhage (Subdra), and vascular dementia (VD) such as Binswanger's disease (Bins). The ND group included patients with Parkinson's disease (PD) as confirmed using appropriate diagnostic guidelines [31], dementia with Lewy body disease (DLB) [32], frontotemporal dementia such as Pick's disease (PiD) [33], progressive supranuclear palsy (PSP) [34], corticobasal degeneration (CBD) [35], and senile dementia with neurofibrillary tangles (SD-NFTs) [36].

2.3. Blood collection

In midmorning (around 10 AM), blood samples were directly collected from the intermediate cubital vein (or if impossible from the femoral vein) of patients and volunteers using a syringe (TERUMO, Tokyo), transferred into tubes with ethylenediaminetetraacetic acid, di-sodium salt (EDTA 2Na), and kept on ice for blood cell count and laboratory biochemical analysis.

The blood samples were centrifuged at 800×g for 20 min at 4°C, and the resulting plasma supernatants were transferred to several Eppendorf tubes. These supernatants were stored at −30°C prior to colorimetric assay and Aβ quantification.

2.4. Biochemical assays

We used a colorimetric kit (ALPCO) to determine ACE activity [37,38] with the synthetic substrate N-hippuryl-l -histidyl-l-leucine following the manufacturer's protocol (normal range 18–55 units). The levels of Aβ1–40 and 1–42 in plasma were determined using a sandwich enzyme-linked immunosorbent assay (ELISA) kit from Immuno-Biological Laboratories Co., Ltd. (Takasaki-Shi, Gunma, Japan).

2.5. Statistical analysis

The significance of the difference between two groups was determined by Student's *t*-test. The level of significance was $p<0.05$ or $p<0.01$.

3. Results

3.1. Measurement of plasma Aβ level and ACE activity

As shown in Table 1, we analyzed 676 samples. The average age of these subjects at sampling was 59.9 ± 21.0 years. The AD group consisted of 147 patients aged 82.8 ± 9.3. The non-AD group consisted of 529 individuals aged 60.1 ± 21.2. The AD patients were statistically significantly older than the non-AD subjects.

Table 2 shows the average levels of Aβ1–40 and 1–42, 1–42/1–40 ratios, and ACE activity for each subgroup and gender. There were no significant differences between genders.

The plasma Aβ1–40 levels in the CN and NB groups were statistically significantly lower than that in the AD group. However, the plasma Aβ1–40 levels in the VP and ND groups were higher than that in the AD group, although the differences were not statistically significant.

Regarding Aβ1–42, only CN and NB males showed statistically significantly lower levels than the AD patients. CN and NB females also

Table 1
Summary of diagnoses of the main neurological subgroups.

Category		*N*	age(average ± SD)
AD	M	35	76.3 ± 8.1
	F	112	84.8 ± 8.7
	Total	147	82.8 ± 9.3
Non-AD	M	193	59.5 ± 20.4
	F	336	60.4 ± 21.7
	Total	529	60.1 ± 21.2
Completely normal	M	73	45.6 ± 18.6
	F	129	43.9 ± 17.5
	Total	202	44.5 ± 17.9
Normal brain (with medication)	M	67	62.7 ± 17.8
	F	136	66.2 ± 18.5
	Total	203	65.1 ± 18.3
Abnormal brain	M	53	74.6 ± 11.8
	F	71	79.5 ± 8.9
	Total	124	77.3 ± 10.5
Vascular problem (CI/CH/SAH/VD/Bins/Subdra)	M	33	77.5 ± 10.3
	F	43	80.7 ± 8.9
	Total	76	79.3 ± 9.5
Neurodegeneration (DLB/PD/PiD/FTD/PSP/CBD/SD-NFT)	M	14	72.1 ± 11.2
	F	19	78.6 ± 8.1
	Total	33	76.0 ± 9.8
Others	M	6	62.8 ± 15.9
	F	9	75.7 ± 10.4
	Total	15	70.5 ± 13.9
Total	M	228	62.1 ± 19.2
	F	448	58.3 ± 21.6
	Total	676	59.9 ± 21.0

N, sample numbers; SD, standard deviation; M, male; F, female; AD, Alzheimer's disease; CI, cerebral infarction; CH, cerebral hemorrhage; SAH, subarachnoid hemorrhage; VD, vascular dementia; Bins, Binswanger's disease; Subdra, subdural hemorrhage; DLB, dementia with Lewy body disease; PD, Parkinson's disease; PiD, Pick's disease; FTD, frontotemporal dementia; PSP, progressive supranuclear palsy; CBD, corticobasal degeneration; SD-NFT, senile dementia with neurofibrillary tangles.

Table 2
Aβ1–40 and 1–42, 1–42/1–40 ratios, and ACE activity for each subgroup.

NTV		Aβ1–40	Aβ1–42	Aβ1–42/1–40	ACE units
		pmol/μl	pmol/μl	(%)	
AD	M	96.9 ± 69.6	7.4 ± 18.3	5.3 ± 7.0	39.4 ± 15.0
	F	115.4 ± 139.0	21.8 ± 108.0	5.5 ± 12.1	39.0 ± 14.3
	Total	111.0 ± 126.0	17.5 ± 94.9	5.5 ± 11.1	39.1 ± 14.4
Non-AD	M	72.7 ± 76.1	5.7 ± 36.9	3.6 ± 7.8	36.6 ± 13.2
	F	73.4 ± 62.3**	5.6 ± 39.8*	3.1 ± 6.9*	37.0 ± 13.5
	Total	73.1 ± 67.6**	5.6 ± 38.8*	3.3 ± 7.2**	37.1 ± 13.6
Completely normal	M	52.1 ± 14.8**	1.7 ± 3.6*	2.8 ± 4.4*	36.7 ± 13.0
	F	61.9 ± 64.4**	4.8 ± 33.4	2.9 ± 6.9*	36.6 ± 11.3
	Total	58.4 ± 52.3**	3.7 ± 26.8	2.8 ± 6.1**	36.6 ± 11.9
Normal brain (with medication)	M	63.6 ± 24.8**	1.6 ± 4.5*	2.1 ± 3.4**	38.8 ± 13.2
	F	75.4 ± 69.5**	6.8 ± 53.2	2.8 ± 7.7*	39.6 ± 13.7
	Total	71.5 ± 58.8**	5.1 ± 43.7	2.5 ± 6.6**	39.4 ± 13.5
Abnormal brain	M	112.4 ± 134.2	16.3 ± 69.5	6.5 ± 13.0	33.8 ± 13.3
	F	90.4 ± 33.5	4.7 ± 8.8	4.3 ± 4.8	33.6 ± 15.9*
	Total	99.5 ± 91.8	9.7 ± 46.6	5.3 ± 9.3	34.3 ± 15.8**
Vascular problem (CI/CH/SAH/VD/Bins/Subdra)	M	121.1 ± 173.9	21.1 ± 88.1**	6.4 ± 10.0	35.8 ± 12.5
	F	91.3 ± 29.0	4.3 ± 4.7**	4.4 ± 4.6	35.0 ± 15.4
	Total	103.8 ± 114.6	11.3 ± 57.2**	5.2 ± 7.4	35.3 ± 14.1
Neurodegeneration (DLB/PD/PiD/FTD/PSP/CBD/SD-NFT)	M	107.6 ± 36.3	14.3 ± 36.2	9.6 ± 21.3	36.1 ± 16.0
	F	84.0 ± 45.3	5.8 ± 15.8	4.0 ± 6.4	28.6 ± 16.7**
	Total	93.6 ± 42.9	9.2 ± 25.9	6.3 ± 14.4	29.8 ± 16.4**
Others	M	87.3 ± 24.7	2.8 ± 2.4	2.8 ± 2.4	30.7 ± 8.1
	F	99.9 ± 24.4	4.5 ± 1.6	4.6 ± 1.3	37.7 ± 15.7
	Total	94.8 ± 24.4	3.8 ± 2.0	4.0 ± 2.0	34.9 ± 13.3
Total	M	76.4 ± 75.5	5.9 ± 34.7	3.8 ± 7.7	37.1 ± 13.5
	F	70.3 ± 63.8	5.5 ± 41.9	2.9 ± 7.0	37.4 ± 12.8
	Total	72.9 ± 69.1	5.7 ± 38.9	3.3 ± 7.3	37.3 ± 13.1

*$p<0.05$,** $p<0.01$ compared with AD group.
N, sample numbers; SD, standard deviation; M, male; F, female; AD, Alzheimer's disease; CI, cerebral infarction; CH, cerebral hemorrhage; SAH, subarachnoid hemorrhage; VD, vascular dementia; Bins, Binswanger's disease; Subdra, subdural hemorrhage; DLB, dementia with Lewy body disease; PD, Parkinson's disease; PiD, Pick's disease; FTD, frontotemporal dementia; PSP, progressive supranuclear palsy; CBD, corticobasal degeneration;SD-NFT, senile dementia with neurofibrillary tangles.

showed lower Aβ1–42 levels than AD patients, but the difference was not statistically significant. A gender difference was observed in the VP group; the males showed a higher Aβ1–42 level than the females. Although the Aβ1–42/1–40 ratios of the VP and ND groups did not differ significantly from that of the AD group, those of the CN and ND groups were lower than that of the AD group.

Comparisons of ACE activity among the groups showed that the ACE activity of the AD group was higher than that of other groups, although this difference did not reach statistical significance AD females showed a statistically significantly higher ACE activity than ND females. Moreover, the female ND subjects showed a lower ACE activity than the CN and NB females.

We plotted the ACE-induced Aβ1–42 to 1–40 conversion efficiencies, Aβ1–42/1–40 ratios, and ACE activities of the non-AD (Supplemental Figs. 1a, b) and AD (Supplemental Figs. 1c, d) groups. We did not observe any marked differences between these groups for these parameters.

3.2. ACE activity and aging

As shown in Table 1, female AD patients were much older than the females of other groups. We placed age at sampling on the horizontal axis and plotted the ratios of Aβ1–42/1–40 (Supplemental Figs. 2a, b) and ACE activity along the vertical axis (Supplemental Figs. 2c, d). From these graphs, no significant tendencies were evident.

On correction for age by excluding samples from subjects under 64 years of age at sampling Table 3a , the average age of males in the various groups was almost the same whereas AD females remained significantly older than the females of other groups. In terms of ACE activity, however, no conformity was evident either with or without correction for sampling age.

In view of animal studies showing that ACE activity tends to decrease with age, the ACE activities of the subgroups were compared

Table 3a
ACE activity for each subgroup of subjects over 65 years old.

Category		*N*	Age	ACE units
AD	M	33	77.2 ± 7.4	39.9 ± 15.2
	F	108	85.7 ± 7.4	38.6 ± 14.2
	Total	141	83.7 ± 8.3	38.9 ± 14.4
Non-AD	M	94	77.0 ± 7.9	38.2 ± 13.0
	F	163	79.5 ± 7.7	37.5 ± 14.9
	Total	257	78.6 ± 7.8	37.7 ± 14.2
Completely normal	M	13	75.5 ± 9.7	41.7 ± 13.3
	F	18	74.9 ± 8.2	44.0 ± 9.1
	Total	31	75.1 ± 8.7	43.0 ± 10.9
Normal brain (with medication)	M	36	75.9 ± 7.1	40.8 ± 11.5
	F	78	80.0 ± 7.4	39.8 ± 14.0
	Total	114	78.4 ± 7.5	40.1 ± 13.2
Abnormal brain	M	45	78.3 ± 8.0	35.0 ± 13.6
	F	67	80.7 ± 7.4	33.0 ± 15.9*
	Total	112	79.8 ± 7.7	33.8 ± 15.0**
Vascular problem (CI/CH/SAH/VD/Bins/Subdra)	M	30	79.6 ± 8.1	36.9 ± 12.6
	F	42	81.3 ± 8.0	34.9 ± 15.5
	Total	72	80.7 ± 7.9	35.8 ± 15.0
Neurodegeneration (DLB/PD/PiD/FTD/PSP/CBD/SD-NFT)	M	12	75.7 ± 7.4	32.2 ± 16.7
	F	18	79.7 ± 6.7	28.5 ± 17.2**
	Total	30	78.1 ± 7.0	29.3 ± 16.9**
Others	M	3	74.3 ± 11.2	34.6 ± 10.1
	F	7	80.1 ± 6.1	33.4 ± 14.4
	Total	10	78.1 ± 7.0	33.7 ± 12.7
Total	M	127	77.0 ± 7.6	38.6 ± 13.6
	F	271	82.0 ± 8.2	37.9 ± 14.6
	Total	398	80.4 ± 8.3	38.1 ± 14.3

*$p<0.05$,** $p<0.01$ compared with AD group.
N, sample numbers; SD, standard deviation; M, male; F, female; AD, Alzheimer's disease; CI, cerebral infarction; CH, cerebral hemorrhage; SAH, subarachnoid hemorrhage; VD, vascular dementia; Bins, Binswanger's disease; Subdra, subdural hemorrhage; DLB, dementia with Lewy body disease; PD, Parkinson's disease; PiD, Pick's disease; FTD, frontotemporal dementia; PSP, progressive supranuclear palsy; CBD, corticobasal degeneration; SD-NFT, senile dementia with neurofibrillary tangles.

Table 3b
The ACE activity of each of the subgroups was compared from 50 years upward in decade increments.

Category	Sex	*N*	51–60 (*N*:ACEa ± SD)	61–70 (*N*:ACEa ± SD)	71–80 (*N*:ACEa ± SD)	81– (*N*:ACEa ± SD)
AD	M	35	1:35	7:40.5 ± 15.0	17:33.8 ± 11.6	10:48.5 ± 17.4
	F	112	1:51	7:36.4 ± 18.1	22:36.0 ± 13.2	82: 39.9 ± 14.3
Non-AD	M	127	20:31.9 ± 9.3	40:35.8 ± 11.7	32:39.8 ± 14.5	35:37.0 ± 12.5*
	F	223	45:37.0 ± 11.0	38:41.0 ± 14.2	62:38.7 ± 17.1	78:35.0 ± 13.5*
Completely normal	M	25	8:34.3 ± 8.0	9:36.0 ± 13.8	4:46.3 ± 11.8	4:44.7 ± 10.0
	F	42	18:36.6 ± 11.0	14:43.3 ± 10.9	4:44.7 ± 4.3	6:38.9 ± 11.4
Medication with	M	51	8:31.8 ± 10.4	18:35.3 ± 11.0	14:39.7 ± 14.0	11:44.5 ± 8.5
normal brain	F	110	23:36.1 ± 10.8	18:38.7 ± 16.8	32:40.4 ± 17.5	37:38.8 ± 11.1
Abnormal brain	M	51	4:27.4 ± 9.8	13:36.4 ± 11.9	14:38.1 ± 16.1	20:31.4 ± 12.1**
	F	71	4:43.6 ± 13.2	6:37.6 ± 13.0	26:37.3 ± 20.2	35:32.5 ± 12.1**
Vascular problem	M	33	2:21.4 ± 6.0	7:33.7 ± 13.2	8:43.0 ± 15.6	16:34.6 ± 9.3*
	F	43	1:39	5:38.3 ± 14.6	15:37.3 ± 20.2	22:32.5 ± 12.1*
Neurodegeneration	M	14	2:28.7 ± 15.8	3:42.4 ± 14.5	6:31.5 ± 15.5	3:16.3 ± 16.8*
	F	19	1:30	1:34	8:30.2 ± 12.4	9:26.4 ± 21.9*
Others	M	4	0	3:36.8 ± 6.8	0	1:24
	F	9	2:53.0 ± 11.3	0	3:42.6 ± 17.4	4:26.5 ± 8.1
Total	M	162	21:32.1 ± 9.1	47:36.5 ± 12.1	49:37.7 ± 13.8	45:40.0 ± 14.3
	F	335	46:37.3 ± 11.2	45:40.3 ± 14.7	84:38.1 ± 16.2	160:37.5 ± 14.1

*$p<0.05$,** $p<0.01$ compared with AD group.
N, sample numbers; SD, standard deviation; M, male; F, female; AD, Alzheimer's disease.

from 50 years upward in increments of 10 years (Table 3b). All the subgroups were analyzed together with the AD group, and interestingly, several findings in the oldest group (over 81) were statistically significant. The ND group showed the lowest ACE activity, but both genders of the VP group showed statistically lower ACE activities than the AD group. This tendency was also noted in a larger subgroup, AbB. Furthermore, the non-AD group also showed a lower ACE activity than the AD group. However, the ACE activities of the CN and NB groups were not significantly different from that of the AD group. Overall, the tendency was for ACE activity to increase with age, except in the ND group in which ACE activity decreased with age.

As shown in Table 4, after further dividing the subgroups into four smaller groups according to ACE activity (ACE<30, 30≦<50, 50≦<70, 70≦), we calculated the average age at sampling. In the case of the AD group, we also considered onset age. As shown in Table 1, the AD group was the oldest on average. When classified in terms of ACE activity, the group with the highest activity (70≦) was the oldest at both onset and sampling ages among the ACE activity groups and this difference was statistically significant. The CN group showed a similar trend, whereas the other groups did not.

Finally, as shown in Fig. 1a, b and Table 5, onset age correlated with ACE activity. In male subjects, the 61–70 onset age group showed the lowest ACE activity among the onset age groups. However, in female subjects, the 51–60 onset age group showed a lower ACE activity and the 61–70 onset age group showed a significantly lower ACE activity than the 71–80 onset age group. The number of patients in the younger group was insufficient; however, the columns in the figure form a dip with 61–70 years around the bottom. That is, the later the AD onset, the higher the ACE activity.

4. Discussion

As ACE degrades Aβ1–42 to Aβ1–40 via dipeptidase activity [13] and breaks up Aβ into small fragments [11,12], we were able to investigate the relationships of Aβ1–42 and Aβ1–40 levels with ACE activity using the plasma from the AD and non-AD groups. In addition, ACE activity was assessed as a possible AD risk factor.

Peripheral ACE levels and ACE activities are affected by I/D polymorphism [14–19]. In individuals harboring this polymorphism, ACE activity in the brain may be associated with that in peripheral blood. However, in reports showing that I/D polymorphism in the ACE genome affects peripheral blood ACE level [15,17,19,39] and ACE activity [16,40], I allele carriers were found to have low ACE levels and ACE activities. In previously published I/D analyses, the I allele was shown to be a risk factor for AD [21–23]. I/D polymorphism would likely affect the regulation of ACE activity not only in peripheral organs but also in the central nervous system (CNS), and if Aβ degeneration in the brain is diminished, an I allele carrier with a low ACE activity could develop early-onset AD. In this study, we did not carry out an ACE I/D allele analysis, which was unfortunate because our AD patients over 81 years with a high ACE activity might have carried the D allele. We will perform this analysis in the future using materials from our Fukushimura Brain Bank [41].

In this study, we originally considered that a low ACE activity could inhibit the degradation of Aβ1–42 and lead to AD. We found however that a low ACE activity was associated with early-onset AD. Our finding that older AD patients showed a higher ACE activity indicates that a low ACE activity may advance age at onset. Unfortunately, we could not examine a sufficient number of samples from patients 60 years and younger, but this will be rectified in the future. To date, there have been no reports on ACE activity and the age at AD onset, and our analysis of peripheral blood represents a giant step forward in elucidating this relationship.

Regarding the relationship between ACE activity and age, there have been a few studies using animal models that showed that this activity decreases with age, but little is known about this relationship in humans [27–30]. It is not clear from our data (Supplemental Figs. 2c, d) whether ACE activity is associated with age. As shown in Table 3b, although there were no clear trends for subjects under 80 years, ACE activity was statistically significantly the highest in the oldest subjects (over 81 years) with significant differences established in the ND, AbB and VP groups. In this study, we did not focus on the relationship between age and plasma ACE activity, but we will investigate this association using a larger population in the near future. AD patients over 81 years of age showed the highest ACE activity. Having a high ACE activity might delay the onset of AD in individuals predisposed to developing it. Table 4 shows that subjects with the highest ACE activity were significantly older in the AD group as well as the CN group. In the AD group, the onset age was also (bottom part of the column in brackets) significantly earlier. Fig. 1a and b shows the AD group subdivided according to the onset age in decades (horizontal axis) with ACE activity plotted on the vertical axis. As noted in the figures, the bars form a U shape with the 61–70 onset age group for male subjects and at the 51–60 age group for female subjects showing the lowest points. The younger-onset female patients included those with sporadic AD in which there may have been some risk or a strong trigger

Table 4
Comparison of 4 smaller groups divided according to ACE activity (ACE<30, 30≦<50, 50≦<70, 70≦).

Category \ ACE activity (units)		<30	30≦<50	50≦<70	70≦
AD	**N**	44	73	25	5
	Age	81.4 ± 9.69	84.0 ± 8.33	80.8 ± 11.23	87.8 ± 2.17
		**	*	**	
	(onset)	(75.2 ± 11.31)	(75.2 ± 9.16)	(75.2 ± 11.68)	(78.4 ± 3.85)
		*		*	
Non-AD	**N**	157	285	78	9
	Age	59.5 ± 20.62	59.5 ± 21.62	62.7 ± 20.81	56.9 ± 23.02
Completely normal	**N**	61	111	30	0
	Age	42.0 ± 14.00	44.0 ± 18.00	52.3 ± 20.79	
		*	*		
Normal brain (with medication)	**N**	47	118	33	5
	Age	63.0 ± 16.00	66.0 ± 18.00	66.7 ± 20.68	51.6 ± 25.8
Abnormal brain	**N**	49	57	15	3
	Age	77.9 ± 11.81	77.6 ± 9.75	74.9 ± 9.13	77.7 ± 4.16
Vascular problem (CI/CH/SAH/ VD/Bins/Subdra)	**N**	27	37	10	2
	Age	79.6±10.65	80.1 ± 8.80	76.8 ± 9.39	76.0 ± 4.24
Neurodegeneration (DLB/PD/PiD/FTD /PSP/CBD/SD-NFT)	**N**	16	13	3	1
	Age	77.3 ± 9.75	74.2 ± 10.92	74.3 ± 7.23	81
Others	**N**	6	7	2	0
	Age	72.2 ± 20.86	70.4 ± 8.34	66.0 ± 8.49	
Total	**N**	201	358	103	14
	Age	64.0 ± 21.00	65.0 ± 22.00	67.0 ± 20.00	71.0 ± 23.44

*$p<0.05$,** $p<0.01$ compared with AD group.

N, sample numbers; SD, standard deviation; M, male; F, female; AD, Alzheimer's disease; CI, cerebral infarction; CH, cerebral hemorrhage; SAH, subarachnoid hemorrhage; VD, vascular dementia; Bins, Binswanger's disease; Subdra, subdural hemorrhage; DLB, dementia with Lewy body disease; PD, Parkinson's disease; PiD, Pick's disease; FTD, frontotemporal dementia; PSP, progressive supranuclear palsy; CBD, corticobasal degeneration; SD-NFT, senile dementia with neurofibrillary tangles.

leading to AD development, such as harboring the apolipoprotein E (apoE) 4 allele. On the other hand, the strongest risk of sporadic senile-type AD is aging and this is likely related to ACE activity. That is, this younger-onset-associated risk factor is much more stronger than ACE activity in senile AD patients over 60 years whose high ACE activity is associated with a delayed onset due to the degradation of Aβ.

The reason that we had such a large number of subjects in the oldest age group may be due to the fact that the Japanese live longer than people of any other country. With rates of longevity increasing worldwide, the number of AD patients will also increase greatly. Under such circumstances, the regulation of ACE activity will become an important issue and the use of ACE inhibitors for medication of hypertension and heart failure should be reconsidered.

This study showed that peripheral ACE activity did not correlate with Aβ1–42/1–40 ratio and that old age correlated with high ACE activity in AD. Therefore, what exactly is the relationship between peripheral Aβ1-42 and Aβ1-40 levels, and age? A previous report suggested that peripheral Aβ1-42 and Aβ1-40 levels do not change with age in nondemented people who lack apoE 4, although Aβ1–40 level does decrease with age in nondemented apoE 4 carriers [42]. As in our previous report, the onset of AD among our Japanese patients usually occurred after the age of 75. Aβ1–42 is not soluble and exists in the brain in an aggregate form. A high ACE activity, however, allows it to be pumped out after its conversion to Aβ1–40 and dipeptides. Therefore, peripheral Aβ1–40 level might reflect the regulation of Aβ1–42 in the brain as a result of ACE activity. Pyramidal cells in the cerebral cortex express ACE and its expression is up-regulated in AD patients [43–45], although the ACE levels in the brains of our AD patients were low [13]. In other reports, ACE levels in the peripheral blood and CSF of AD and DLB patients are similar to those of normal controls [46], and ACE activity in the CSF of PSP, PD, and AD patients is decreased [47]. However, the relationship between peripheral blood and CSF in terms of ACE level or ACE activity has not been reported. In any case, these analyses provide a starting point for examining associations of these factors with onset age.

Our findings in this study were as follows: 1) AD patients with a higher ACE activity were at a more advanced age at onset, suggesting that peripheral plasma ACE activity affects the age at onset of AD. This might represent a serious problem because many elderly people are prescribed ACE inhibitors. In view of this finding, it might be worth reconsidering certain forms of hypertension therapy. 2) The level of Aβ1–40 in the peripheral blood of AD patients was significantly higher than that of the CN or NB group. Moreover, the Aβ1–42 level was also higher, although not significantly so. 3) There was no significant correlation between Aβ1–42/1–40 ratio and ACE activity in either the

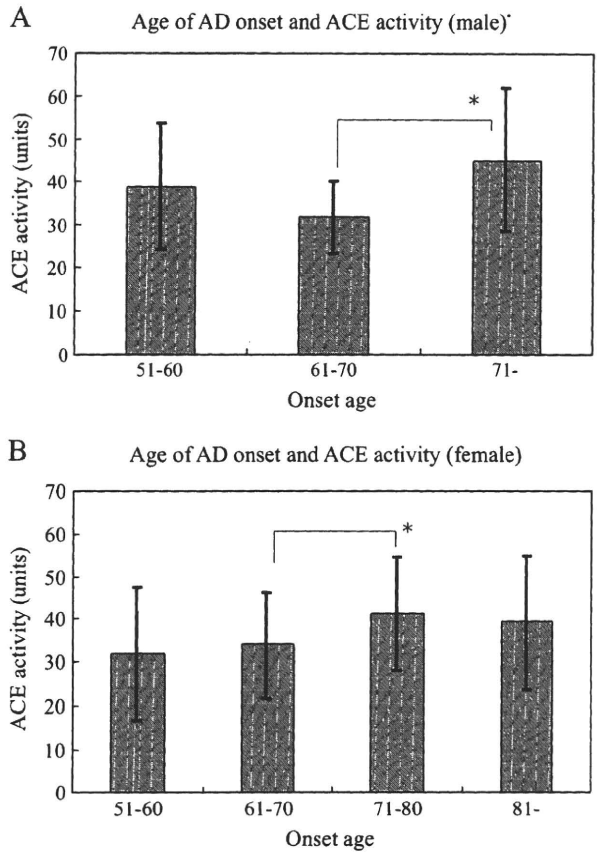

Fig. 1. *N* at the bottom of each column indicates the number of samples. ACE activity (units) averages with SD are shown on the columns which represent onset ages grouped according to decade. In this subgroup comparison, * indicates a statistical significance of 5%. a) The onset age of AD male patients is correlated with ACE activity (units). b) The onset age of AD female patients is correlated with ACE activity (units). For females, only two AD patients under 50 years old were available (shadowed in Table 5, where the range in ACE activity is shown), so these were not included in the figure, even though their measured ACE activity was the highest recorded.

AD or non-AD group. It has been shown that the major source of ACE in the blood comes from the kidney and lung [28,30]. However, our present study has shown that blood ACE activity is associated with the age at onset of AD, suggesting that brain ACE may enter into the blood circulation and increase the ACE level in blood. It may be reasonable to assume that later-onset AD is associated with a higher brain ACE level, which in turn may be associated with a high blood ACE level. As shown in our previous report, the human brain produces ACE, but it is unknown whether the amount of ACE generated would significantly alter the ACE level in peripheral blood.

Supplementary materials related to this article can be found online at doi:10.1016/j.jns.2010.09.030.

Table 5
Age of AD onset and ACE activity.

Males				Females			
Age at AD onset	*N*	ACE activity (average ± SD)		Age at AD onset	*N*	ACE activity (average ± SD)	
-50	0			-50	2	55.1 ± 5.3	
51–60	9	39.0 ± 14.9		51–60	7	32 ± 15.3	
61–70	11	31.6 ± 8.6	*	61–70	19	34 ± 12.2	*
71-	15	45.0 ± 16.8		71–80	49	41.2 ± 13.4	
				81-	35	39.2 ± 15.7	

*$p<0.05$,** $p<0.01$ compared with AD group.

Acknowledgements

This study was supported by a grant from the Japan Health Sciences Foundation (Research on Publicly Essential Drugs and Medical Devices), a grant from the Program for the Promotion of Fundamental Studies in Health Sciences of the National Institute of Biomedical Innovation (NIBRO), and a grant from the Ministry of Health, Labor and Welfare of Japan (Comprehensive Research on Aging and Health Grant H20-007).

References

[1] Walsh DM, Klyubin I, Fadeeva JV, Cullen WK, Anwyl R, Wolfe MS, et al. Naturally secreted oligomers of amyloid beta protein potently inhibit hippocampal long-term potentiation in vivo. Nature 2002;416:535–9.
[2] Borchelt DR, Thinakaran G, Eckman CB, Lee MK, Davenport F, Ratovitsky T, et al. Familial Alzheimer's disease-linked presenilin 1 variants elevate Abeta1–42/1–40 ratio in vitro and in vivo. Neuron 1996;17:1005–13.
[3] Citron M, Westaway D, Xia W, Carlson G, Diehl T, Levesque G, St George Hyslop P, Selkoe DJ, et al. Mutant presenilins of Alzheimer's disease increase production of 42-residue amyloid beta-protein in both transfected cells and transgenic mice. Nat Med 1997;3:67–72.
[4] Heese K, Akatsu H. Alzheimer's disease–an interactive perspective. Curr Alzheimer Res 2006;3:109–21.
[5] Zou K, Michikawa M. Angiotensin-converting enzyme as a potential target for treatment of Alzheimer's disease: inhibition or activation? Rev Neurosci 2008;19: 203–12.
[6] Eckman EA, Eckman CB. Abeta-degrading enzymes: modulators of Alzheimer's disease pathogenesis and targets for therapeutic intervention. Biochem Soc Trans 2005;33:1101–5.
[7] Iwata N, Tsubuki S, Takaki Y, Shirotani K, Lu B, Gerard NP, et al. Metabolic regulation of brain Abeta by neprilysin. Science 2001;292:1550–2.
[8] Miller BC, Eckman EA, Sambamurti K, Dobbs N, Chow KM, Eckman CB, et al. Amyloid-beta peptide levels in brain are inversely correlated with insulysin activity levels in vivo. Proc Nat Acad Sci USA 2003;100:6221–6.
[9] Farris W, Mansourian S, Chang Y, Lindsley L, Eckman EA, Frosch MP, et al. Insulin-degrading enzyme regulates the levels of insulin, amyloid beta-protein, and the beta-amyloid precursor protein intracellular domain in vivo. Proc Nat Acad Sci USA 2003;100:4162–7.
[10] Mueller-Steiner S, Zhou Y, Arai H, Roberson ED, Sun B, Chen J, et al. Antiamyloidogenic and neuroprotective functions of cathepsin B: implications for Alzheimer's disease. Neuron 2006;51:703–14.
[11] Hemming ML, Selkoe DJ. Amyloid beta-protein is degraded by cellular angiotensin-converting enzyme (ACE) and elevated by an ACE inhibitor. J Biol Chem 2005;280: 37644–50.
[12] Hu J, Igarashi A, Kamata M, Nakagawa H. Angiotensin-converting enzyme degrades Alzheimer amyloid beta-peptide (A beta); retards A beta aggregation, deposition, fibril formation; and inhibits cytotoxicity. J Biol Chem 2001;276: 47863–8.
[13] Zou K, Yamaguchi H, Akatsu H, Sakamoto T, Ko M, Mizoguchi K, et al. Angiotensin-converting enzyme converts amyloid beta-protein 1–42 (Abeta(1–42)) to Abeta (1–40), and its inhibition enhances brain Abeta deposition. J Neurosci 2007;27: 8628–35.
[14] Baghai TC, Binder EB, Schule C, Salyakina D, Eser D, Lucae S, et al. Polymorphisms in the angiotensin-converting enzyme gene are associated with unipolar depression, ACE activity and hypercortisolism. Mol Psychiatry 2006;11:1003–15.
[15] Rigat B, Hubert C, Alhenc-Gelas F, Cambien F, Corvol P, Soubrier F. An insertion/deletion polymorphism in the angiotensin I-converting enzyme gene accounting for half the variance of serum enzyme levels. J Clin Invest 1990;86:1343–6.
[16] Martinez E, Puras A, Escribano J, Sanchis C, Carrion L, Artigao M, et al. Angiotensin-converting enzyme (ACE) gene polymorphisms, serum ACE activity and blood pressure in a Spanish-Mediterranean population. J Hum Hypertens 2000;14:131–5.
[17] Keavney B, McKenzie CA, Connell JM, Julier C, Ratcliffe PJ, Sobel E, et al. Measured haplotype analysis of the angiotensin-I converting enzyme gene. Hum Mol Genet 1998;7:1745–51.
[18] Danilov S, Savoie F, Lenoir B, Jeunemaitre X, Azizi M, Tarnow L, et al. Development of enzyme-linked immunoassays for human angiotensin I converting enzyme suitable for large-scale studies. J Hypertens 1996;14:719–27.
[19] Tiret L, Rigat B, Visvikis S, Breda C, Corvol P, Cambien F, et al. Evidence, from combined segregation and linkage analysis, that a variant of the angiotensin I-converting enzyme (ACE) gene controls plasma ACE levels. Am J Hum Genet 1992;51:197–205.
[20] Gainer JV, Stein CM, Neal T, Vaughan DE, Brown NJ. Interactive effect of ethnicity and ACE insertion/deletion polymorphism on vascular reactivity. Hypertension 2001;37:46–51.
[21] Elkins JS, Douglas VC, Johnston SC. Alzheimer disease risk and genetic variation in ACE: a meta-analysis. Neurology 2004;62:363–8.
[22] Lehmann DJ, Cortina-Borja M, Warden DR, Smith AD, Sleegers K, Prince JA, et al. Large meta-analysis establishes the ACE insertion–deletion polymorphism as a marker of Alzheimer's disease. Am J Epidemiol 2005;162:305–17.
[23] Wang B, Jin F, Yang Z, Lu Z, Kan R, Li S, et al. The insertion polymorphism in angiotensin-converting enzyme gene associated with the APOE epsilon 4 allele increases the risk of late-onset Alzheimer disease. J Mol Neurosci 2006;30:267–71.

[24] Kehoe PG, Katzov H, Feuk L, Bennet AM, Johansson B, Wiman B, et al. Haplotypes extending across ACE are associated with Alzheimer's disease. Hum Mol Genet 2003;12:859–67.
[25] Meng Y, Baldwin CT, Bowirrat A, Waraska K, Inzelberg R, Friedland RP, et al. Association of polymorphisms in the Angiotensin-converting enzyme gene with Alzheimer disease in an Israeli Arab community. Am J Hum Genet 2006;78: 871–7.
[26] Heyman A, Peterson B, Fillenbaum G, Pieper C. The consortium to establish a registry for Alzheimer's disease (CERAD). Part XIV: demographic and clinical predictors of survival in patients with Alzheimer's disease. Neurology 1996;46:656–60.
[27] Challah M, Nadaud S, Philippe M, Battle T, Soubrier F, Corman B, et al. Circulating and cellular markers of endothelial dysfunction with aging in rats. Am J Physiol 1997;273:H1941–8.
[28] Yosipiv IV, Dipp S, el-Dahr SS. Ontogeny of somatic angiotensin-converting enzyme. Hypertension 1994;23:369–74.
[29] Mooradian AD, Lieberman J. Age-related decrease in serum angiotensin converting enzyme activity: the role of thyroidal status and food intake. J Gerontol 1990;45:B24–7.
[30] Costerousse O, Allegrini J, Huang H, Bounhik J, Alhenc-Gelas F. Regulation of ACE gene expression and plasma levels during rat postnatal development. Am J Physiol 1994;267:E745–53.
[31] Tolosa E, Wenning G, Poewe W. The diagnosis of Parkinson's disease. Lancet Neurol 2006;5:75–86.
[32] Lippa CF, Duda JE, Grossman M, Hurtig HI, Aarsland D, Boeve BF, et al. DLB and PDD boundary issues: diagnosis, treatment, molecular pathology, and biomarkers. Neurology 2007;68:812–9.
[33] McKhann GM, Albert MS, Grossman M, Miller B, Dickson D, Trojanowski JQ. Clinical and pathological diagnosis of frontotemporal dementia: report of the Work Group on Frontotemporal Dementia and Pick's Disease. Arch Neurol 2001;58:1803–9.
[34] Nath U, Ben-Shlomo Y, Thomson RG, Lees AJ, Burn DJ. Clinical features and natural history of progressive supranuclear palsy: a clinical cohort study. Neurology 2003;60: 910–6.
[35] Doran M, du Plessis DG, Enevoldson TP, Fletcher NA, Ghadiali E, Larner AJ. Pathological heterogeneity of clinically diagnosed corticobasal degeneration. J Neurol Sci 2003;216:127–34.
[36] Yamada M. Senile dementia of the neurofibrillary tangle type (tangle-only dementia): neuropathological criteria and clinical guidelines for diagnosis. Neuropathology 2003;23:311–7.
[37] Hurst PL, Lovell-Smith CJ. Optimized assay for serum angiotensin-converting enzyme activity. Clin Chem 1981;27:2048–52.
[38] Neels HM, Scharpe SL, van Sande ME, Verkerk RM, Van Acker KJ. Improved micromethod for assay of serum angiotensin converting enzyme. Clin Chem 1982;28:1352–5.
[39] Biller H, Zissel G, Ruprecht B, Nauck M, Busse Grawitz A, Muller-Quernheim J. Genotype-corrected reference values for serum angiotensin-converting enzyme. Eur Respir J 2006;28:1085–90.
[40] Soubrier F, Martin S, Alonso A, Visvikis S, Tiret L, Matsuda F, et al. High-resolution genetic mapping of the ACE-linked QTL influencing circulating ACE activity. Eur J Hum Genet 2002;10:553–61.
[41] Akatsu H, Takahashi M, Matsukawa N, Ishikawa Y, Kondo N, Sato T, et al. Subtype analysis of neuropathologically diagnosed patients in a Japanese geriatric hospital. J Neurol Sci 2002;196:63–9.
[42] Pomara N, Shao B, Wisniewski T, Mehta PD. Decreases in plasma A beta 1–40 levels with aging in non-demented elderly with ApoE-epsilon 4 allele. Neurochem Res 1998;23:1563–6.
[43] Savaskan E, Hock C, Olivieri G, Bruttel S, Rosenberg C, Hulette C, et al. Cortical alterations of angiotensin converting enzyme, angiotensin II and AT1 receptor in Alzheimer's dementia. Neurobiol Aging 2001;22:541–6.
[44] Barnes NM, Cheng CH, Costall B, Naylor RJ, Williams TJ, Wischik CM. Angiotensin converting enzyme density is increased in temporal cortex from patients with Alzheimer's disease. Eur J Pharmacol 1991;200:289–92.
[45] Miners JS, Ashby E, Van Helmond Z, Chalmers KA, Palmer LE, Love S, et al. Angiotensin-converting enzyme (ACE) levels and activity in Alzheimer's disease, and relationship of perivascular ACE-1 to cerebral amyloid angiopathy. Neuropathol Appl Neurobiol 2008;34:181–93.
[46] Nielsen HM, Londos E, Minthon L, Janciauskiene SM. Soluble adhesion molecules and angiotensin-converting enzyme in dementia. Neurobiol Dis 2007;26:27–35.
[47] Zubenko GS, Volicer L, Direnfeld LK, Freeman M, Langlais PJ, Nixon RA. Cerebrospinal fluid levels of angiotensin-converting enzyme in Alzheimer's disease, Parkinson's disease and progressive supranuclear palsy. Brain Res 1985;328:215–21.

Journal of Neuroscience Research

Journal of Neuroscience Research 88:3547–3554 (2010)

Amyloid β Accelerates Phosphorylation of Tau and Neurofibrillary Tangle Formation in an Amyloid Precursor Protein and Tau Double-Transgenic Mouse Model

Yusuke Seino,[1] Takeshi Kawarabayashi,[2]* Yasuhito Wakasaya,[2] Mitsunori Watanabe,[2] Ayumi Takamura,[2] Yukiko Yamamoto-Watanabe,[2] Tomoko Kurata,[3] Koji Abe,[3] Masaki Ikeda,[4] David Westaway,[5] Tetsuro Murakami,[6] Peter St. George Hyslop,[6] Etsuro Matsubara,[2] and Mikio Shoji[2]

[1]Department of General Medicine, Mutsu General Hospital, Mutsu, Japan
[2]Department of Neurology, Hirosaki University Graduate School of Medicine, Hirosaki, Japan
[3]Department of Neurology, Okayama University Graduate School of Medicine and Dentistry, Okayama, Japan
[4]Department of Neurology, Gunma University Graduate School of Medicine, Maebashi, Japan
[5]Centre for Prions and Protein Folding Diseases, University of Alberta, Edmonton, Alberta, Canada
[6]Canada Centre for Research in Neurodegenerative Diseases, University of Toronto, Toronto, Ontario, Canada

In Alzheimer's disease, Aβ deposits are considered the initial cardinal events that induce tauopathy secondarily. However, the relationship between Aβ amyloidosis and tauopathy has not been determined in detail. We produced double transgenic mice, 2×TgTau$^{+/-}$APP$^{+/-}$, by mating Tg2576 mice that exhibit Aβ amyloidosis and TgTauP301L mice that show tauopathy, and statistically analyzed the effect of Aβ accumulation on tauopathy. There was no significant difference in the progression of Aβ accumulation among 2×TgTau$^{+/-}$APP$^{+/-}$ and 1×TgTau$^{-/-}$APP$^{+/-}$, and tau accumulation among 2×TgTau$^{+/-}$APP$^{+/-}$ and 1×TgTau$^{+/-}$APP$^{-/-}$. The appearance rates of phosphorylated tau developing in neurons and processes were significantly accelerated in 2×TgTau$^{+/-}$APP$^{+/-}$ mice compared with those in 1×TgTau$^{+/-}$APP$^{-/-}$ mice at 23 months of age. Accumulation of phosphorylated and confomationally altered tau and GSK3β in neuronal processes was accelerated in the white matter in 2×TgTau$^{+/-}$APP$^{+/-}$. The level of phosphorylated tau in the sarkosyl-insoluble fraction was increased in 2×TgTau$^{+/-}$APP$^{+/-}$ brains compared with that in 1×TgTau$^{+/-}$APP$^{-/-}$ brains. Thus, Aβ amyloid partially enhances tauopathy through accumulation of insoluble, phosphorylated, and conformationally changed tau in neuronal cytoplasm and processes in the late stage.

Key words: Alzheimer's disease; double transgenic mouse; neurofibrillary tangles

Alzheimer's disease (AD) brains are invariably characterized by two pathological features, initial Aβ amyloidosis by extracellular deposition of Aβ and subsequent intracellular accumulation of neurofibrillary tangles (NFTs) comprising abnormal aggregates of phosphorylated tau. Aβ cascade from Aβ deposits to the final appearance of tauopathy and neuronal cell losses is the major hypothesis that explains all steps in the pathogenesis of AD. Soluble Aβ oligomers are considered the cardinal molecules that adversely affect synaptic structures and plasticity (Hardy, 2009). Tauopathy is present in sporadic frontotemporal dementia such as progressive supranuclear palsy and corticobasal degeneration and caused by MAPT gene mutation itself in FTDP-17 (Hutton et al., 1998). Other types of diseases such as brain amyloids of familial British dementia (Ghiso et al., 2001) and lysosomal disorders of Niemann-Pick disease type C also induce numerous NFTs (Love et al., 1995). Because JNPL3 mice expressing double APP and tau mutations exhibited substantial enhanced NFT pathology in the limbic system and

Contract grant sponsor: Ministry of Health, Labor and Welfare of Japan; Contract grant number: 19390233 (to M.S.); Contract grant number: 19590976 (to T.Ka.); Contract grant number: 18590968 (to E.M.); Contract grant sponsor: Ministry of Education, Culture, Sports, Science and Technology, Japan (to M.S.); Contract grant sponsor: The Mochida Memorial Foundation for Medical and Pharmaceutical Research (to M.W.); Contract grant sponsor: Hirosaki University Institutional Research (to M.S.).

*Correspondence to: Takeshi Kawarabayashi, Department of Neurology, Institute of Brain Science, Hirosaki University Graduate School of Medicine 5 Zaifucho, Hirosaki 036-8562, Japan.
E-mail: tkawara@cc.hirosaki-u.ac.jp

Received 12 May 2010; Revised 5 August 2010; Accepted 17 August 2010

Published online 8 October 2010 in Wiley Online Library (wileyonlinelibrary.com). DOI: 10.1002/jnr.22516

olfactory cortex (Lewis et al., 2001), investigations into mechanisms underlying Aβ induced tauopathy have been facilitated. Accumulation of phosphorylated tau was enhanced around senile plaque cores (Tomidokoro et al., 2001). Injection of Aβ42 fibrils or brain Aβ extracts into the brains of the tau transgenic mice models caused increases in the number of NFTs (Götz et al., 2001). Administration of Aβ antibodies cleared Aβ deposits and delayed subsequent tauopathy in a 3×Tg-AD mouse model (Oddo et al., 2004). Blocking Aβ42 or Aβ oligomer accumulation delayed the onset and progression of tau pathology (Oddo et al., 2008). Reduction of both soluble Aβ and tau levels have been suggested as necessary to rescue cognitive impairment in 3×Tg-AD model mice (Oddo et al., 2006a). In contrast, augmenting tau levels did not modulate the onset or progression of Aβ pathology (Oddo et al., 2007). Thus, a unidirectional mechanism from Aβ amyloids to tauopathy is suggested in transgenic mouse models. However, follow-up of a phase I trial of immunization with Aβ42 did not prevent clinical progression of dementia, tauopathy, or neuronal cell loss, even though it resulted in the clearance of amyloid plaques (Holmes et al., 2008). These findings have facilitated further clarification of the precise mechanisms underlying induction of tauopathy by Aβ amyloidosis.

We have established a tauopathy model mouse expressing 2N4R human tauP301L (TgTauP301L), which develops a florid pathology that includes numerous pretangles, NFTs, and glial fibrillary tangles (GFTs) in the frontotemporal areas of the cerebrum, accompanied by gliosis, neuronal loss, and cerebral atrophy. Accumulated tau was hyperphosphorylated, conformationally changed, ubiquitinated, and sarkosyl insoluble. These mice exhibited impairment in hippocampus-dependent and -independent behavioral paradigms and showed substantial phenotypic variation and a spectrum of pathologies similar to that observed in FTDP-17 patients (Murakami et al., 2006). Here, we generated double transgenic mice, $2\times TgTau^{+/-}APP^{+/-}$, by mating Tg2576 mice that exhibit marked Aβ deposits (Kawarabayashi et al., 2004) with TgTauP301L mice in order to analyze how Aβ amyloids induces tauopathy. Progression of deposits of Aβ, phosphorylated and conformatinally changed tau, NFTs, GFT, and phenotypic variation were compared among $2\times TgTau^{+/-}APP^{+/-}$, $1\times Tau^{+/-}APP^{-/-}$, $1\times TgTau^{-/-}APP^{+/-}$, and $0\times TgTau^{-/-}APP^{-/-}$ mice. Although there were no significant changes in the progression of Aβ and tau deposits from 8 to 16 months of age, the presence of phosphorylated and conformationally changed tau in dystrophic neurites around senile plaques and neuropil threads and the appearance of pretangles and NFTs were significantly enhanced in $2\times TgTau^{+/-}APP^{+/-}$ at 23 months of age. Based on these findings, the acceleration of tauopathy by Aβ amyloidosis was considered slow and not very strong, requiring a long incubation period during which phosphorylation, conformational change, and insolubilization of tau occurred.

MATERIALS AND METHODS

Transgenic Mouse Models

To generate double transgenic mice expressing tauP301L and βAPP KM670/671NL, TgTauP301L maintained in the FVB/N strain were mated with Tg2576 mice maintained in the B6/SJL strain and defined as $2\times TgAPP^{+/-}Tau^{+/-}$. Heterozygote F1 littermates of TgTauP301 and Tg2576 were used for all experiments to analyze uniform genetic background mice as FVB/B6/SJL. Each genotypic strain was $2\times TgTau^{+/-}APP^{+/-}$ expressing human 2N4R tauP301L and βAPP KM670/671NL, $1\times TgTau^{+/-}APP^{-/-}$, $1\times TgTau^{-/-}APP^{+/-}$, and $0\times TgTau^{-/-}APP^{-/-}$, which was the wild FVB/B6/SJL mouse expressing only endogenous mouse APP and tau. In total 124 mice were examined. Twenty-three $2\times TgTau^{+/-}APP^{+/-}$ (3 mice at 8 months of age, 4 mice at 12 months, 6 mice at 16 months, and 8 mice at 23 months), 62 $1\times TgTau^{+/-}APP^{-/-}$ (7 mice at 8 months, 15 mice at 12 months, 27 mice at 16 months, and 13 mice at 23months), 16 $1\times TgTau^{-/-}APP^{+/-}$ (1 mouse at 8 months, 1 mouse at 12 months, 5 mice at 16 months, and 9 mice at 23 months), and 23 $0\times TgTau^{-/-}APP^{-/-}$ (16 mice at 8 months, 1 mouse at 12 months, 19 mice at 16 months, and 4 mice at 23 months) were analyzed. All animal experiments were performed according to guidelines established in the Guide for the care and use of laboratory animals and the ethical committee of Hirosaki University.

Immunostaining

After mice were sacrificed under ether anesthesia, brains were removed and cut sagitally along the midline. One hemisphere was fixed in 4% paraformaldehyde with 0.1 M phosphate buffer (pH 7.6) for 8 hr and embedded in paraffin. Five-micrometer-thick sections were prepared for immunostaining and Gallyas-Braak silver stain. Sections were immersed in 0.5% periodic acid to block intrinsic peroxidase and treated with 99% formic acid for 3 min. Microwave pretreatment was used for AT8 staining. After blocking with 5% normal goat or horse serum in 50 mM phosphate-buffered saline (pH 7.4) containing 0.05% Tween 20 and 4% Block Ace (Snow Brand, Sapporo, Japan), sections were incubated overnight with primary antibodies. Specific labeling was visualized by Vectastain Elite ABC kit (Vector, Burlingame, CA). Tissue sections were counterstained with hematoxylin. The following antibodies were used in this study: tau-154, against amino acids 154–168 of human tau441 that specifically detect human tau (1:200); HT7. against amino acids 159–163 of human tau441 that specifically detect human tau (1:500; Innogenetics, Gent, Belgium); CP27, against all forms of human tau (1:500); TAU-5, against amino acids of human tau441 that detects both human and mouse tau (1:1,000; Abcam, Cambridge, MA); MC1, against early epitope of confomationally changed tau (1:400); PS199, against phosphorylated tau at serine199 (1:500); CP13, against phosphorylated tau at serine202 (1:400); AT8, against phosphorylated tau at serine202/threonine205 (1:400; Innogenetics); anti-PT231/PS235, against phosphorylated tau at threonine231/serine235 (1:500); PHF-1, against phosphorylated tau at serine396/serine404 (1:400); anti-PS413, against phosphorylated tau at serine413 (1:100);

Ab9204, against N-terminal aspartate of Aβ (0.1 μg/ml); and anti-GSK3β antibody (1:100) were used (Tomidokoro et al., 2001).

Western Blot

The other half of the mouse brain was weighed and homogenized using a motor-driven Teflon glass homogenizer for 20 strokes in 9 volumes of Tris-saline buffer (TS) with protease inhibitors (TS inhibitors 50 mM Tris-HCl and 150 mM NaCl, pH 7.6, with protease inhibitor cocktail; Complete; Roche Diagnostics, Indianapolis, IN). The homogenate was centrifuged at 55,000 rpm for 60 min at 4°C, and the supernatant was analyzed as the TS-soluble fraction. After washing with 10 volumes of TS with protease inhibitors, the pellet was homogenized again in 4 volumes of 1% sarkosyl in TS inhibitors, incubated on ice for 30 min, and centrifuged at 55,000 rpm for 60 min at 4°C. The supernatant was analyzed as the sarkosyl-soluble fraction. The pellet was washed twice with 10 volumes of 1% sarkosyl in TS inhibitors, and the remaining pellet was analyzed as the sarkosyl-insoluble fraction. Each sample was boiled at 70°C in SDS sample buffer, separated on 4–12% NuPAGE Bis-Tris Gel (Invitrogen, Carlsbad, CA), and electrotransferred to Immobilon P (Millipore, Bedford, MA) at 100 V for 1.5 hr. The blots were labeled by HT-7, Tau5, PHF-1, AT8, and CP13. The signal intensity of labeled protein using Supersignal (Pierce, Rockford, IL) was quantified by the luminoimage analyzer (LAS 1000-Mini; Fuji Film, Tokyo, Japan).

RESULTS

Appearance of expressed human tauP301L began at 3 months of age in both $2\times TgTau^{+/-}APP^{+/-}$ and $1\times TgTau^{+/-}APP^{-/-}$. With aging, the human tauP301L accumulated progressively and distributed widely from the hippocampus to the cerebral cortices, thalamus, amygdale, striatum, and brainstem. There were no significant differences observed in initiation, distribution, and progression of human tauP301L accumulation between $2\times TgTau^{+/-}APP^{+/-}$ (Fig. 1a–d) and $1\times TgTau^{+/-}APP^{-/-}$ (Fig. 1e–h). Neither brain atrophy nor hydrocephalus was observed in either group. Progressive accumulation of endogenous mouse tau was also detected by TAU-5 immunostaining in relation to the expressed human tauP301L accumulation. There were no significant differences in brain gliosis, neuronal cell loss, behavioral disturbance, or survival between $2\times TgTau^{+/-}APP^{+/-}$ and $1\times TgTau^{+/-}APP^{-/-}$. However, marked accumulation of phosphorylated tau was detected by AT8 immunostaining in the hippocampus and the cerebral cortices in $2\times TgTau^{+/-}APP^{+/-}$ mice compared with $1\times TgTau^{+/-}APP^{-/-}$ mice at 23 months age (Fig. 1l). This accumulated tau was partially labeled by Gallyas silver stain (see Fig. 2x), suggesting the presence of both pretangles and NFTs in the brains of $2\times TgTau^{+/-}APP^{+/-}$ mice at 23 months of age. Phenotypic variations were also recognized in both $2\times TgTau^{+/-}APP^{+/-}$ and $1\times TgTau^{+/-}APP^{-/-}$ like those in TgTauP301L.

Aβ core plaques labeled by Ab9201 appeared from 8 months of age in both $2\times TgTau^{+/-}APP^{+/-}$ and $1\times TgTau^{-/-}APP^{+/-}$. Numbers and distributions were increased with age in both groups. However, there were no differences in the initiation and distribution of Aβ deposits between $2\times TgTau^{+/-}APP^{+/-}$ (Fig. 1q–t) and $1\times TgTau^{-/-}APP^{+/-}$ (Fig. 1u–x). Furthermore, there were no differences in diffuse Aβ plaques at 16–23 months of age in the two group. From 8 months of age, dystrophic neurites around Aβ cores were present (Fig. 2a). The appearance of phosphorylated tau deposits in dystrophic neurites was enhanced in $2\times TgTau^{+/-}APP^{+/-}$ (Fig. 2c) compared with that in $1\times TgTau^{+/-}APP^{-/-}$ (Fig. 2d). These findings suggested that tauopathy does not induce Aβ amyloidosis, but rather Aβ amyloidosis accelerates phosphorylation and tangle formation of accumulated tau.

Then, phosphorylated tau was examined in detail in the brain of a 23-month-old $2\times TgTau^{+/-}APP^{+/-}$ mouse (Fig. 2e,g,h). Numerous neuropil threads were detected by AT8 staining in the cerebral cortex of the brain (Fig. 2g). There were phosphorylated tau-positive, Gallyas silver stain-negative neurites in the cerebral white matter (Fig. 2h), suggesting the presence of pretangles in the neuronal process. There was no apparent correlation between Aβ amyloid cores and NFTs, as shown in Figure 2i,j. Enhanced GSK-3β staining was also observed (Fig. 2k).

Neurons containing phosphorylated tau-positive pretangles were significantly enhanced and 3.7 times more frequently in the $2\times TgTau^{+/-}APP^{+/-}$ (63%, 5/8) compared with $1\times TgTau^{+/-}APP^{-/-}$ (17%, 5/29) at 23 months of age (Table I, $P = 0.0107$: χ^2 test; Graph Pad Prism 5). Glial tangles were also prominent in the brains of $2\times TgTau^{+/-}APP^{+/-}$: 6/8 (75%) of $2\times TgTau^{+/-}APP^{+/-}$ and 11/29 (38%) of $1\times TgTau^{+/-}APP^{-/-}$ mice ($P = 0.06$). However, there was no significant difference in the incidence of GFTs. Thus, Aβ enhances pretangle formation in neurons and processes.

These pretangles were labeled by antibodies against special phosphorylation sites at serine199 (Fig. 2r), at serine202 (Fig. 2s), at serine202/threonine205 (Fig. 2t), at threonine231/serine235 (Fig. 2u), at serine396/serine404 (Fig. 2v), and at serine413 (Fig. 2w), with conformational changes by MC1 (Fig. 2q) and by Gallyas silver staining (Fig. 2x). These findings correspond to those detected in TgTauP301L and patients with Alzheimer's disease or FTDP-17, suggesting that the appearance, severity, and modifications of accumulated tau are more accelerated by Aβ amyloidosis in $2\times TgTau^{+/-}APP^{+/-}$ than in $1\times TgTau^{+/-}APP^{-/-}$ mice.

To confirm the enhancement and acceleration of tau phosphorylation and NFTs formation, we examined the presence and amounts of sarkosyl-insoluble phosphorylated tau in the $2\times TgTau^{+/-}APP^{+/-}$ and $1\times TgTau^{+/-}APP^{-/-}$ 23-month-old mice by Western blot (Fig. 3). In the first Tris buffer-soluble fractions, human-specific tau antibody HT7 labeled the 66-kD bands. TAU-5 demonstrated 66-kD and 55-kD bands. There were no significant differences in the amounts of human and mouse tau in the Tris-soluble brain fractions of the two groups (Fig. 3a). Almost equal amounts of

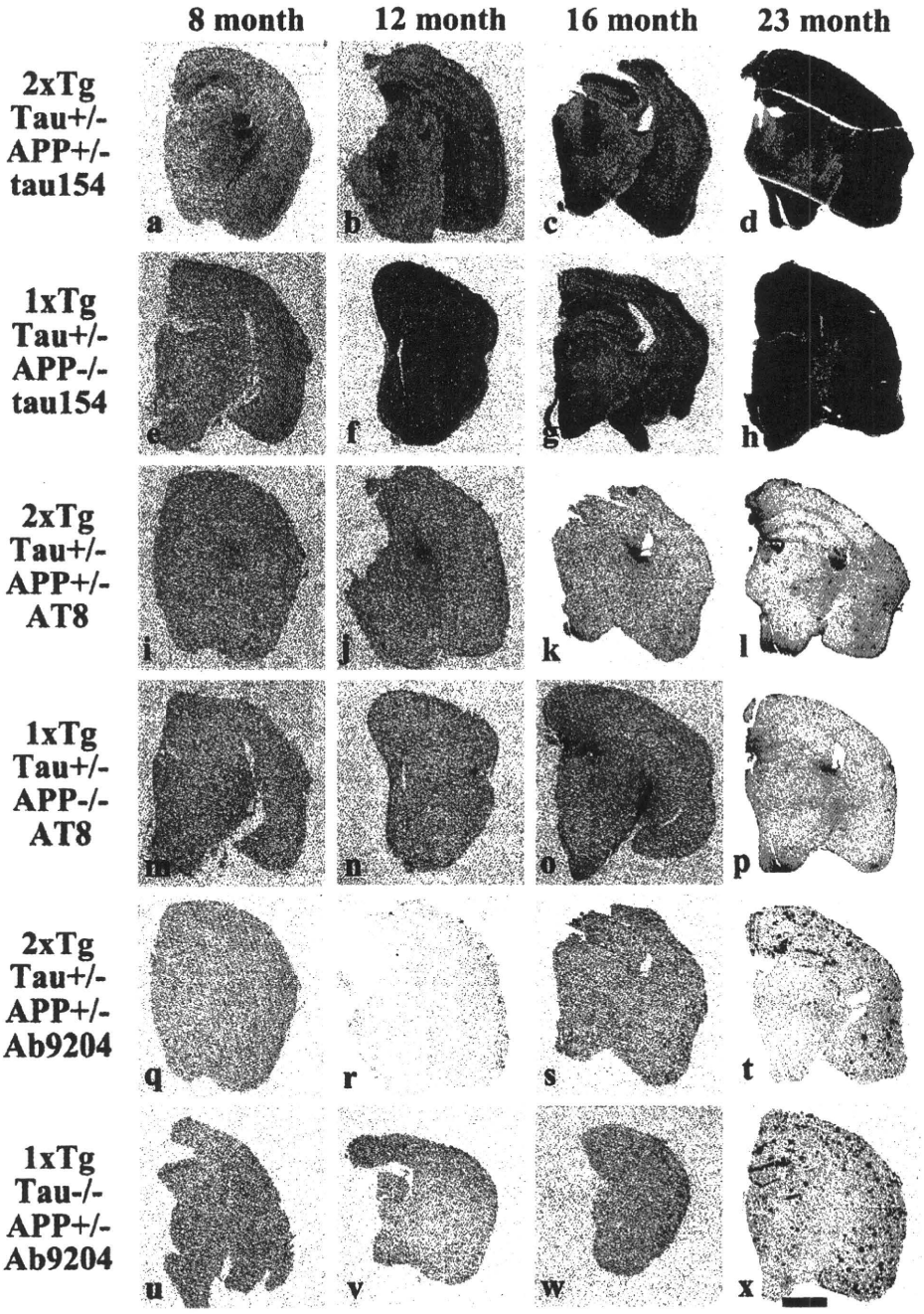

Fig. 1. Time course of accumulation of human tau, phosphorylated tau, and Aβ in 8–23-month-old $2\times TgTau^{+/-}APP^{+/-}$ (**a–d,i–l,q–t**), $1\times Tau^{+/-}APP^{-/-}$ (**e–h,m–p**), and $1\times TgTau^{-/-}APP^{+/-}$ (**u–x**) mice. Mouse sections were stained with tau154 that specifically detects human tau, AT8 for phosphorylated tau at serine202/threonine205, and Ab9204 for Aβ. Scale bar = 800 μm. [Color figure can be viewed in the online issue, which is available at wileyonlinelibrary.com.]

human tau were detected in the sarcosyl-soluble fractions from the brains of both groups (Fig. 3b). However, increased amounts of 66-kD full-length human tauP301L and their 58-kD fragments were increased in the sarkosyl-insoluble brain fraction of $2\times TgTau^{+/-}APP^{+/-}$ compared with those of $1\times TgTau^{+/-}APP^{-/-}$. These

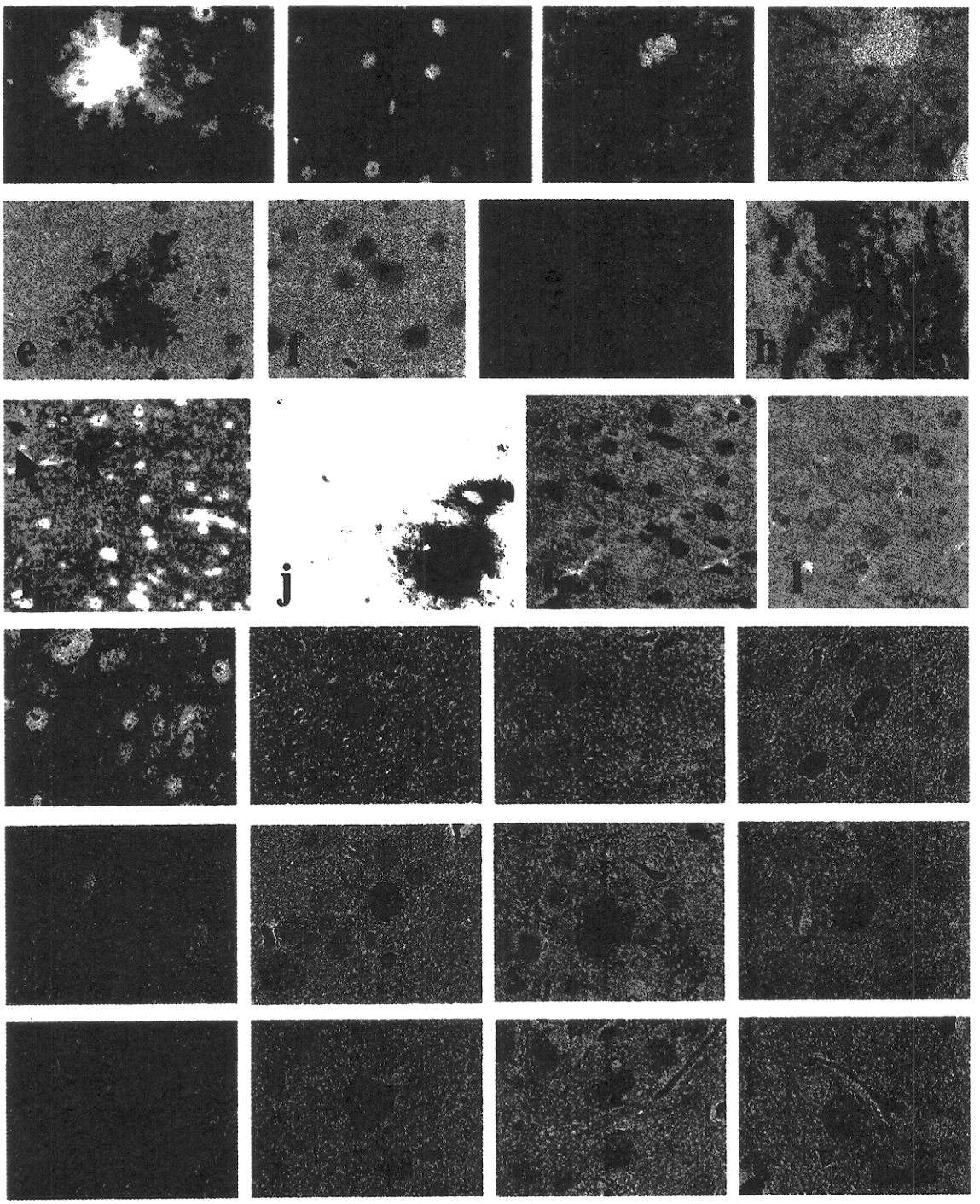

Fig. 2. Immunostaining of $2\times TgTau^{+/-}APP^{+/-}$ (**a,c,e,g–k,m–x**), $1\times TgTau^{+/-}APP^{-/-}$ (**b,f,l**), and $1\times TgTau^{-/-}APP^{+/-}$ (**d**) mice. Sections were stained with tau154 (a,b,i), AT8 (c–h), Ab9204 (j), anti-GSK3β (k,l). Cerebral cortex of $2\times TgTau^{+/-}APP^{+/-}$ was stained anti-tau antibodies; tau-154 (m), HT7 (n), CP27 (o), TAU-5 (p), MC1 (q), anti-PS199 (r), CP13 (s), AT8 (t), anti-PT231/PS235 (u), PHF1 (v), anti-PS413 (w), and Gallyas-Braak stain (x). Scale bar = 12.5 μm. [Color figure can be viewed in the online issue, which is available at wileyonlinelibrary.com.]

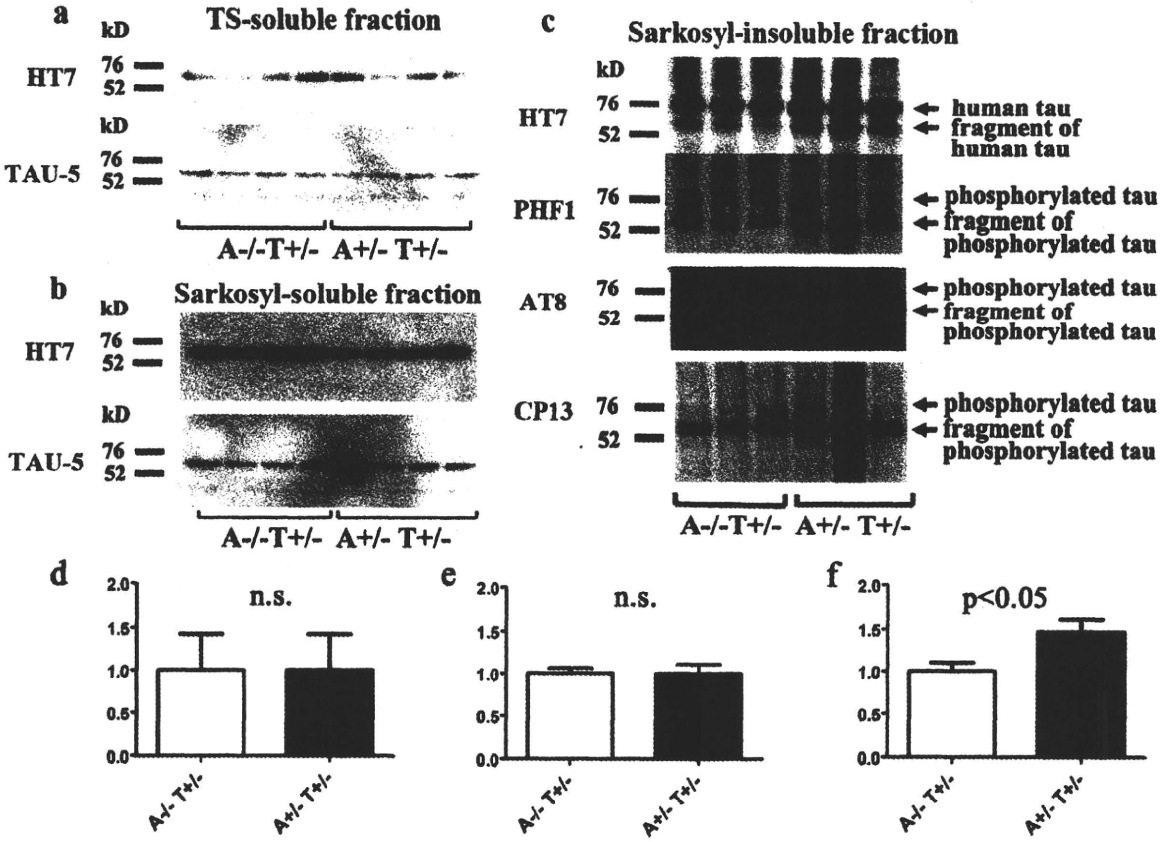

Fig. 3. Western blotting of brain extracts from $2\times TgTau^{+/-}APP^{+/-}$ ($A^{+/-}T^{+/-}$) and $1\times TgTau^{+/-}APP^{-/-}$ ($A^{-/-}T^{+/-}$). **a:** TS-soluble fraction stained with HT7 and TAU-5. **b:** Sarkosyl-soluble fraction stained with HT7 and TAU-5. **c:** Sarcosyl-insoluble fraction stained with HT7, PHF-1, AT8, and CP13. The signal intensity of tau in the sarkosyl-insoluble fraction (**f**) was significantly increased in $2\times TgTau^{+/-}APP^{+/-}$ compared with that in $1\times TgTau^{+/-}APP^{-/-}$; however, that in the TS-soluble fraction (**d**) and sarkosyl-soluble fraction (**e**) did not differ. The mean intensity of the band in $1\times TgTau^{+/-}APP^{-/-}$ is shown as 1.

TABLE I. NFTs and GFTs in $2\times TgTau^{+/-}APP^{+/-}$ and $1\times TgTau^{+/-}APP^{-/-}$

Genotype	$2\times TgTau^{+/-}APP^{+/-}$	$1\times TgTau^{+/-}APP^{-/-}$
Neurofibrillary pretangles	63% (5/8)**	17% (5/29)
Glial fibrillary pretangles	75% (6/8)	38% (11/29)

**$P = 0.0107$.

increased tau isoforms were also labeled by antibody PHF1, AT8, and CP13, suggesting that sarkosyl-insoluble tau is hyperphosphorylated and conformationally changed in the most insoluble brain fractions, which corresponds to those recognized in Alzheimer's disease brains (Fig. 3c). Thus, acceleration of tauopathy in the $2\times TgTau^{+/-}APP^{+/-}$ brain was also detected by biochemical examinations.

DISCUSSION

Both $2\times TgTau^{+/-}APP^{+/-}$ and $1\times TgTau^{+/-}APP^{-/-}$ showed initiation and accumulation of tauP301L starting at 3 months, and those accumulations progressively spread from the hippocampus to the cortices, amygdala, and brainstem. The initial appearance of dystrophic neurites around the core plaques was detected in both mice at the same period of 8 months of age. The number and size of phosphorylated tau were enhanced in dystrophic neurites of $2\times TgTau^{+/-}APP^{+/-}$ mice. Phosphorylated tau-positive pretangles, NFTs, and GFTs and phenotypic variation were also reproduced in both mice. However, the prevalence of mice exhibiting pretangles, NFTs, and phosphorylated tau-positive neuropils was significantly increased in $2\times TgTau^{+/-}APP^{+/-}$ compared with $1\times TgTau^{+/-}APP^{-/-}$ mice at 23 months of age. The distributions of pretangles and NFTs were not correlated with the presence of core plaques. These findings suggest that the presence of Aβ amyloidosis partially enhances the accumulation of phosphorylated tau in neurons and neuronal processes.

Subsequent generation of Aβ plaques and tangles and neurodegeneration have been exhibited by regulatory expression model mice of tauP301L (rTg4510; Spires et al., 2006; Spires-Jones et al., 2008; de Calington et al., 2009) and APPNLI (rTg3696AB; Paulson et al., 2008). In our $2\times TgTau^{+/-}APP^{+/-}$ mice, however, the appearances of pretangles, NFTs, and GFTs were markedly delayed at 23 months of age. Tauopathy was detected at 18 months of age in TgtauP301L, so about a 5-month delay was observed. Florid pathology including brain atrophy, neuronal cell loss, and gliosis detected in TgtauP301L was milder in both $2\times TgTau^{+/-}APP^{+/-}$ and $1\times TgTau^{+/-}APP^{-/-}$ even at 23 months of age. This delay and a milder form of tau pathology were observed in $1\times TgTau^{+/-}APP^{-/-}$, so one possible explanation is that alteration of the genetic background by crossing strains from FBV in TgTauP301L with FVB/B6/SJL occurred in the crossing of double heterozygotes Tg. For this reason, we analyzed many heterozygotes of mice in this study to confirm this phenomenon statistically and to show significant enhancement of tau pathology by Aβ in $2\times TgTau^{+/-}APP^{+/-}$.

Development of Aβ burden was completely identical among $2\times TgTau^{+/-}APP^{+/-}$, $1\times TgTau^{-/-}APP^{+/-}$, and Tg2576. Initial Aβ deposits were detected at 8 months of age, and there was no significant difference in the progressive distribution and density among these three strains. In other double and triple Tg mice, genetically augmented tau levels and hyperphosphorylation in the 3×Tg-AD did not show any effect on the onset and progression of Aβ pathology (Oddo et al., 2007). The somatodendritic tau accumulation is dependent on parenchymal Aβ deposits (Oddo et al., 2009). Aβ-dependent triosephosphate isomerase nitrotyrosination induces glycation and tau fibrillation (Guix et al., 2009). Thus, unidirectional facilitation of tauopathy by Aβ amyloidosis and Aβ oligomer was considered (Oddo et al., 2006b). The initial alteration of Tg2576 brain was Aβ dimers in lipid rafts at 6 months of age, and subsequent accumulation of phosphorylated tau was identified (Kawarabayashi et al., 2004). Because enhancement of pretangles, NFTs and GTFs appeared in the late stage of Aβ burden consisting of many core plaques and diffuse plaques, the acceleration effect of tauopathy by Aβ amyloid is not considered very strong, but the incubation period seems to be long despite previous findings regarding the mutant presenilin-1 effect on APP double Tg mice (Holcomb et al., 1998).

As clearly shown in TgtauP301L, many tau transgenic mice exhibited loss of neurons and synapses. Accumulation of tau in axonal defects was an early event in the brains of AD and APP Tg mice (Stokin et al., 2005). Suppression of tau expression in mice expressing a repressible tauP301L developing progressive NFTs, neuronal cell loss, and behavioral impairments recovered memory function and neuron numbers (Santacruz et al., 2005). Transgenic TAU zebrafish clearly showed that GSK3β-mediated NFT formation actually induces neuronal cell death (Paquet et al., 2009). Neurotoxicity induced by fibrillar Aβ on hippocampal cultured neurons is mediated by tau (Rapoport et al., 2002). There was no neuronal cell loss or synaptic losses at 23 months of age in $2\times TgTau^{+/-}APP^{+/-}$. These findings indicated that an NFT burden more severe than that shown in $2\times TgTau^{+/-}APP^{+/-}$ is necessary to induce neuronal cell loss and that Aβ amyloid fibrils and oligomer were not sufficient to induce this neurodegenerative processes.

Other double transgenic mice obtained by crossing Tg2576 and tau transgenic mice expressing tauG272V, P301L, and R406W showed an increase in tau phosphorylation at serine262 and -422 (Pérez et al., 2005). Lithium, a well-known drug that inhibits GSK-3 activities, reduced tau phosphorylation but did not alter the Aβ load (Caccamo et al., 2007). Injection of Aβ42 fibrils into the brains of tauP301L transgenic mice caused a fivefold increase in the number of NFTs in the amygdala where neurons projected to the injected site, 18 days after Aβ42 injection (Götz et al., 2001). Amyloid induces tauopathy through activation of GSK-3β in APP-V717I × TauP301L mice (Terwel et al., 2008). Tau reduction can block Aβ and excitotoxin-induced neuronal dysfunction (Robertson et al., 2007). All these findings indicate that Aβ might induce NFTs through phosphorylation of tau and formation of conformationally changed tau and GSK3β activation. In accordance with these findings, $2\times TgTau^{+/-}APP^{+/-}$ showed enhanced phosphorylation at serine199, at serine202, at serine202/threonine205, at threonine231/serine235, at serine 396/serine404, and at serine413 and the presence of conformational alteration and argylophilic properties as well as increased expression of GSK-3β. Biochemical analysis further confirmed the histological findings and indicated that this hyperphosphorylated and conformationally changed tau acutully gains insolubility, leading to accumulation of aggregated tau in the sarkosyl-insoluble fraction in the brain.

In summary, enhancement of tauopathy by Aβ may partially initiate pretangle formation in the neuronal processes and cytoplasm. Based on the presence of many pretangles in the cortex, NFTs and GFTs emerged. These findings correspond to conventional neuropathological findings and other reports on AD model mice (LaFerla and Oddo, 2005, Spires-Jones et al., 2009). Our data and these reports support the hypothesis that disturbance of axonal transport of phosphorylated tau in the axons is an early event induced by Aβ amyloid deposition. Further drug development targeting this step would be desirable.

ACKNOWLEDGMENTS

We thank K. Sato, M. Ono, K. Iinuma, Y. Sato, R. Tushima, and I. Shirahama for technical assistance; Dr. TC Saido for generously donating Ab9204; Dr. Peter Davies for CP27, CP13, MC1, and PHF-1 antibodies; and Dr. Koich Ishiguro for tau-154, PS199, anti-PT231/PS235, anti-PS413, anti-GSK3β antibodies.

REFERENCES

Caccamo A, Oddo S, Tran LX, LaFerla FM. 2007. Lithium reduces tau phosphorylation but not Aβ or working memory deficits in a transgenic model with both plaques and tangles. Am J Pathol 170:1669–1675.

de Calignon A, Spires-Jones TL, Pitstick R, Carlson GA, Hyman BT. 2009. Tangle-bearing neurons survive despite disruption of membrane

integrity in a mouse model of tauopathy. J Neuropathol Exp Neurol 68:757–761.

Ghiso JA, Holton J, Miravalle L, Calero M, Lashley T, Vidal R, Houlden H, Wood N, Neubert TA, Rostagno A, Plant G, Revesz T, Frangione B. 2001. Systemic amyloid deposits in familial British dementia. J Biol Chem 276:43909–43914.

Götz J, Chen F, van Dorpe J, Nitsch RM. 2001. Formation of neurofibrillary tangles in P301L tau transgenic mice induced by Aβ42 fibrils. Science 293:1491–1495.

Guix FX, Ill-Raga G, Bravo R, Nakaya T, de Fabritiis G, Coma M, Miscione GP, Villà-Freixa J, Suzuki T, Fernàndez-Busquets X, Valverde MA, de Strooper B, Muñoz FJ. 2009. Amyloid-dependent triosephosphate isomerase nitrotyrosination induces glycation and tau fibrillation. Brain 132:1335–1345.

Hardy J. 2009. The amyloid hypothesis for Alzheimer's disease: a critical reappraisal. J Neurochem 110:1129–1134.

Holcomb L, Gordon MN, McGowan E, Yu X, Benkovic S, Jantzen P, Wright K, Saad I, Mueller R, Morgan D, Sanders S, Zehr C, O'Campo K, Hardy J, Prada CM, Eckman C, Younkin S, Hsiao K, Duff K. 1998. Accelerated Alzheimer-type phenotype in transgenic mice carrying both mutant amyloid precursor protein and presenilin 1 transgenes. Nat Med 4:97–100.

Holmes C, Boche D, Wilkinson D, Yadegarfar G, Hopkins V, Bayer A, Jones RW, Bullock R, Love S, Neal JW, Zotova E, Nicoll JA. 2008. Long-term effects of Aβ42 immunization in Alzheimer's disease: follow-up of a randomised, placebo-controlled phase I trial. Lancet 372:216–223.

Hutton M, Lendon CL, Rizzu P, Baker M, Froelich S, Houlden H, Pickering-Brown S, Chakraverty S, Isaacs A, Grover A, Hackett J, Adamson J, Lincoln S, Dickson D, Davies P, Petersen RC, Stevens M, de Graaff E, Wauters E, van Baren J, Hillebrand M, Joosse M, Kwon JM, Nowotny P, Che LK, Norton J, Morris JC, Reed LA, Trojanowski J, Basun H, Lannfelt L, Neystat M, Fahn S, Dark F, Tannenberg T, Dodd PR, Hayward N, Kwok JB, Schofield PR, Andreadis A, Snowden J, Craufurd D, Neary D, Owen F, Oostra BA, Hardy J, Goate A, van Swieten J, Mann D, Lynch T, Heutink P. 1998. Association of missense and 5′-splice-site mutations in tau with the inherited dementia FTDP-17. Nature 393:702–705.

Kawarabayashi T, Shoji M, Younkin LH, Wen-Lang L, Dickson DW, Murakami T, Matsubara E, Abe K, Ashe KH, Younkin SG. 2004. Dimeric amyloid β protein rapidly accumulates in lipid rafts followed by apolipoprotein E and phosphorylated tau accumulation in the Tg2576 mouse model of Alzheimer's disease. J Neurosci 24:3801–3809.

LaFerla FM, Oddo S. 2005. Alzheimer's disease: Aβ, tau and synaptic dysfunction. Trends Mol Med 11:170–176.

Lewis J, Dickson DW, Lin WL, Chisholm L, Corral A, Jones G, Yen SH, Sahara N, Skipper L, Yager D, Eckman C, Hardy J, Hutton M, McGowan E. 2001. Enhanced neurofibrillary degeneration in transgenic mice expressing mutant tau and APP. Science 293:1487–1491.

Love S, Bridges LR, Case CP. 1995. Neurofibrillary tangles in Niemann-Pick disease type C. Brain 118:119–129.

Murakami T, Paitel E, Kawarabayashi T, Ikeda M, Chishti MA, Janus C, Matsubara E, Sasaki A, Kawarai T, Phinney AL, Harigaya Y, Horne P, Egashira N, Mishima K, Hanna A, Yang J, Iwasaki ,K, Takahashi M, Fujiwara M, Ishiguro K, Bergeron C, Carlson GA, Abe K, Westaway D, St. George-Hyslop P, Shoji M. 2006. Cortical neuronal and glial pathology in TgTauP301L transgenic mice: neuronal degeneration, memory disturbance, and phenotypic variation, Am J Pathol 169:1365–1375.

Oddo S, Billings L, Kesslak JP, Cribbs DH, LaFerla FM. 2004. Aβ immunotherapy leads to clearance of early, but not late, hyperphosphorylated tau aggregates via the proteasome. Neuron 43:321–332.

Oddo S, Vasilevko V, Caccamo A, Kitazawa M, Cribbs DH, LaFerla FM. 2006a. Reduction of soluble Aβ and tau, but not soluble Aβ alone, ameliorates cognitive decline in transgenic mice with plaques and tangles. J Biol Chem 281:39413–39423.

Oddo S, Caccamo A, Tran L, Lambert MP, Glabe CG, Klein WL, LaFerla FM. 2006b. Temporal profile of amyloid-β (Aβ) oligomerization in an in vivo model of Alzheimer disease. A link between Aβ and tau pathology. J Biol Chem 281:1599–1604.

Oddo S, Caccamo A, Cheng D, Jouleh B, Torp R, LaFerla FM. 2007. Genetically augmenting tau levels does not modulate the onset or progression of Aβ pathology in transgenic mice. J Neurochem 102:1053–1063.

Oddo S, Caccamo A, Tseng B, Cheng D, Vasilevko V, Cribbs DH, LaFerla FM. 2008. Blocking Aβ42 accumulation delays the onset and progression of tau pathology via the C terminus of heat shock protein70-interacting protein: a mechanistic link between Aβ and tau pathology. J Neurosci 28:12163–12175.

Oddo S, Caccamo A, Cheng D, LaFerla FM. 2009. Genetically altering Aβ distribution from the brain to the vasculature ameliorates tau pathology. Brain Pathol 19:421–430.

Paquet D, Bhat R, Sydow A, Mandelkow EM, Berg S, Hellberg S, Fälting J, Distel M, Köster RW, Schmid B, Haass C. 2009. A zebrafish model of tauopathy allows in vivo imaging of neuronal cell death and drug evaluation. J Clin Invest 119:1382–1395.

Paulson JB, Ramsden M, Forster C, Sherman MA, McGowan E, Ashe KH. 2008. Amyloid plaque and neurofibrillary tangle pathology in a regulatable mouse model of Alzheimer's disease. Am J Pathol 173:762–772.

Pérez M, Ribe E, Rubio A, Lim F, Morán MA, Ramos PG, Ferrer I, Isla MT, Avila J. 2005. Characterization of a double (amyloid precursor protein-tau) transgenic: tau phosphorylation and aggregation. Neuroscience 130:339–347.

Rapoport M, Dawson HN, Binder LI, Vitek MP, Ferreira A. 2002. Tau is essential to β-amyloid-induced neurotoxicity. Proc Natl Acad Sci U S A 99:6364–6369.

Roberson ED, Scearce-Levie K, Palop JJ, Yan F, Cheng IH, Wu T, Gerstein H, Yu GQ, Mucke L. 2007. Reducing endogenous tau ameliorates amyloid β-induced deficits in an Alzheimer's disease mouse model. Science 316:750–754.

Santacruz K, Lewis J, Spires T, Paulson J, Kotilinek L, Ingelsson M, Guimaraes A, DeTure M, Ramsden M, McGowan E, Forster C, Yue M, Orne J, Janus C, Mariash A, Kuskowski M, Hyman B, Hutton M, Ashe KH. 2005. Tau suppression in a neurodegenerative mouse model improves memory function. Science 309:476–481.

Spires TL, Orne JD, SantaCruz K, Pitstick R, Carlson GA, Ashe KH, Hyman BT. 2006. Region-specific dissociation of neuronal loss and neurofibrillary pathology in a mouse model of tauopathy. Am J Pathol 168:1598–1607.

Spires-Jones TL, de Calignon A, Matsui T, Zehr C, Pitstick R, Wu HY, Osetek JD, Jones PB, Bacskai BJ, Feany MB, Carlson GA, Ashe KH, Lewis J, Hyman BT. 2008. In vivo imaging reveals dissociation between caspase activation and acute neuronal death in tangle-bearing neurons. J Neurosci 28:862–867.

Spires-Jones TL, Stoothoff WH, de Calignon A, Jones PB, Hyman BT. 2009. Tau pathophysiology in neurodegeneration: a tangled issue. Trends Neurosci 32:150–159.

Stokin GB, Lillo C, Falzone TL, Brusch RG, Rockenstein E, Mount SL, Raman R, Davies P, Masliah E, Williams DS, Goldstein LS. 2005. Axonopathy and transport deficits early in the pathogenesis of Alzheimer's disease. Science 307:1282–1288.

Terwel D, Muyllaert D, Dewachter I, Borghgraef P, Croes S, Devijver H, Van Leuven F. 2008. Amyloid activates GSK-3β to aggravate neuronal tauopathy in bigenic mice. Am J Pathol 172:786–798.

Tomidokoro Y, Ishiguro K, Harigaya Y, Matsubara E, Ikeda M, Park JM, Yasutake K, Kawarabayashi T, Okamoto K, Shoji M. 2001. Aβ amyloidosis induces the initial stage of tau accumulation in APP(Sw) mice. Neurosci Lett 299:169–172.

Journal of Neuroscience Research

Journal of Neuroscience Research 89:576–584 (2011)

Factors Responsible for Neurofibrillary Tangles and Neuronal Cell Losses in Tauopathy

Yasuhito Wakasaya,[1] Takeshi Kawarabayashi,[1]* Mitsunori Watanabe,[1] Yukiko Yamamoto-Watanabe,[1] Ayumi Takamura,[1] Tomoko Kurata,[2] Tetsuro Murakami,[2] Koji Abe,[2] Kiyofumi Yamada,[3] Koichi Wakabayashi,[4] Atsushi Sasaki,[5] David Westaway,[6] Peter St. George Hyslop,[7] Etsuro Matsubara,[1] and Mikio Shoji[1]

[1]Department of Neurology, Institute of Brain Science, Hirosaki University Graduate School of Medicine, Hirosaki, Japan
[2]Department of Neurology, Okayama University Graduate School of Medicine, Dentistry and Pharmaceutical Sciences, Okayama, Japan
[3]Department of Neuropsychopharmacology and Hospital Pharmacy, Nagoya University Graduate School of Medicine, Nagoya, Japan
[4]Department of Neuropathology, Institute of Brain Science, Hirosaki University Graduate School of Medicine, Hirosaki, Japan
[5]Department of Pathology, Saitama Medical University, Saitama, Japan
[6]Centre for Prions and Protein Folding Diseases, 204 Environmental Engineering Building, University of Alberta, Edmonton, Alberta, Canada
[7]Centre for Research in Neurodegenerative Diseases, Departments of Medicine (Neurology) and Laboratory Medicine and Pathobiology, University of Toronto, Toronto, Ontario, Canada

TgTauP301L mice that overexpress the mutant human tauP301L present in FTDP-17 reproduce neurofibrillary tangles (NFTs), neuronal cell losses, memory disturbance, and substantial phenotypic variation. To demonstrate factors responsible for NFT formation and neuronal cell losses, sets of TgTauP301L for comparison with or without NFTs and neuronal cell losses were studied with oligonucleotide microarrays. Gene expressions were altered in biological pathways, including oxidative stress, apoptosis, mitochondrial fatty acid betaoxidation, inflammatory response pathway, and complement and coagulation cascade pathways. Among 24 altered genes, increased levels of apolipoprotein D (ApoD) and neuronal PAS domain protein 4 (Npas4) and decreased levels of doublecortin (DCX) and potassium channel, voltage-gated, shaker-related subfamily, β member 1 (Kcnab1) were found in the TgTauP301L with NFTs and neuronal cell losses, Alzheimer's brains, and tauopathy brains. Thus, many biological pathways and novel molecules are associated with NFT formation and neuronal cell losses in tauopathy brains.

Key words: tauopathy; Apo D; Npas4; DCX; Kcnab1

Alzheimer's disease (AD) brains are invariably characterized by two pathological features: initial Aβ amyloidosis by extracellular deposition of Aβ, and subsequent tauopathy with intracellular accumulation of neurofibrillary tangles (NFTs) comprising abnormal aggregates of phosphorylated tau. Aβ cascade from Aβ deposits to the final appearance of NFTs and neuronal cell losses is the major hypothesis that explains all steps in the pathogenesis of AD (Hardy, 2009). Although soluble Aβ oligomers are cardinal molecules that adversely affect synaptic structures and plasticity, leading to memory disturbance, neuronal cell loss is closely related to the presence of NFTs (Spires-Jones et al., 2009). Accumulation of tau in axonal defects is an early event in AD brain and in APP transgenic mouse (Stokin et al., 2005). Suppression of tau expression in mice expressing a repressible tauP301L and developing progressive NFTs, neuronal cell losses, and behavior

Contract grant sponsor: Ministry of Health, Labor and Welfare of Japan (to M.S.); Contract grant sponsor: Ministry of Education, Culture, Sports, Science and Technology, Japan; Contract grant number: 19390233 (to M.S.); Contract grant number: 19590976 (to T.K.); Contract grant number: 18590968 (to E.M.); Contract grant sponsor: The Mochida Memorial Foundation for Medical and Pharmaceutical Research (to M.W.); Contract grant sponsor: Hirosaki University Institutional Research (to M.S.).

*Correspondence to: Dr. Takeshi Kawarabayashi, Department of Neurology, Institute of Brain Science, Hirosaki University Graduate School of Medicine, 5 Zaifucho, Hirosaki 036-8562, Japan.
E-mail: tkawara@cc.hirosaki-u.ac.jp

Received 1 September 2010; Revised 8 November 2010; Accepted 9 November 2010

Published online 13 January 2011 in Wiley Online Library (wileyonlinelibrary.com). DOI: 10.1002/jnr.22572

impairments recovered memory function and neuron numbers (Santacruz et al., 2005). However, once NFTs are formed, these features are irreversible (Holmes et al., 2008). Transgenic tau zebrafish have clearly shown that GSK3β-mediated NFT formation actually induces neuronal cell losses (Paquet et al., 2009). These findings support the hypothesis that tauopathy is the critical event in neuronal cell losses in AD and frontotemporal dementia (FTD) patients. In FTD and parkinsonism linked to chromosome 17 (FTDP-17), there is large variation in the clinical and neuropathological features of disease among patients showing the same mutation within a family. We recently established a tauopathy model mouse expressing 2N4R human tauP301L, developing florid pathology, including numerous pretangles, NFTs, glial fibrillary tangles (GFTs), gliosis, and neuronal cell losses in the frontotemporal areas of the cerebrum accompanied by cerebral atrophy (TgTauP301L; Murakami et al., 2006). As expected, TgTauP301L also showed variation in phenotypic manifestation. Given that the genetic modifiers or associated molecules are clarified by comparison between individuals showing severe pathology including numerous NFTs and neuronal cell losses and those with only pretangles, study of the variance both in families with FTDP-17 and in our mouse model can contribute to clarifying the pathological cascade from accumulation of phosphorylated tau to NFT formation and final neuronal cell losses. On the basis of this hypothesis, here we analyzed oligonucleotide microarrays to determine the mRNA expression profile in TgTauP301L with and without tau pathology and showed the alterations of biological pathways and novel proteins associated with NFTs and neuronal cell losses.

MATERIALS AND METHODS

Subjects

TgTauP301L were back-crossed to FVB/N strain mice for more than six generations to obtain a uniform genetic background. Two sets of TgTauP301L consisted of the 517 mouse with human tau accumulation (Fig. 1Ba–e) and the 512 mouse showing extensive NFTs and neuronal cell losses (Fig. 1Bf–j), which were compared at 24 months of age, as well as the 739 mouse with only human tau accumulation (Fig. 1Aa,b, Bk–o) and the 736 mouse showing extensive NFTs and neuronal cell losses (Fig. 1Ac,d, Bp–t), which were compared at 26 months of age, using oligonucleotide microarrays. After mice were sacrificed under ether anesthesia, the sagittal half of the brain was immediately frozen at −80°C for Western blot and microarray analysis, and the other half of the brain was analyzed histologically. An additional 185 TgTauP301L between 3 months and 30 months of age, 52 nontransgenic control littermates (3–30 months old), and autopsy brains from five patients with Alzheimer's disease (ages 65–81 years), five patients with tauopathy [two frontotemporal dementia (FTD), two corticobasal degeneration, and one supranuclear palsy (ages 71–78 years)], and five normal controls (ages 71–91 years) were examined by immunostaining and biochemical analysis.

Target RNA Preparation and Oligonucleotide Array Expression Analysis

Total RNAs from two sets of mouse brains were isolated using the Trizol reagent (Invitrogen, Carlsbad, CA) and purified with a RNeasy Mini Kit (Qiagen, Valencia, CA). The One-Cycle cDNA synthesis kit from Affymetrix was used to synthesize cDNA from 2 μg of total RNA. Biotinylated cRNA was generated from the cDNA using the IVT Labeling Kit (Affymetrix, Santa Clara, CA), followed by fragmentation of the cRNA target using a fragmentation buffer for 35 min at 94°C before chip hybridization, then 15 μg of fragmented cRNA was added to a hybridization cocktail (0.05 μg/μl fragmented cRNA, 50 pM control oligonucleotide B2, 1.5 pM *BioB*, 5 pM *BioC*, 25 pM *BioD*, and 100 pM *cre* hybridization controls, 0.1 mg/ml herring sperm DNA, 0.5 mg/ml acetylated BSA, 100 mM MES, 1 M Na^+, 20 mM EDTA, 0.01% Tween 20). Ten micrograms of cRNA from each sample was hybridized to a separate oligonucleotide array (Affymetrix Mouse Genome 430 2.0) for 16 hr at 45°C in the GeneChip Hybridization Oven 640. The arrays were washed and stained with streptavidin phycoerythrin in the GeneChip Fluidics Station 450. Then, the arrays were scanned with a GeneChip Scanner 3000.

Data Analysis

The Affymetrix GeneChip Microarray Suite 5.0 (MAS5) algorithm was used to generate signal values and detection calls (present, absent or marginal). Only genes that had a "present" or "marginal" detection call on all four chips were chosen, with 24,330 identified for further analysis from a total of 45,101 genes. Ratios of changes in gene expression were obtained by the differences between 517 and 512 and between 739 and 736. Gene expression ratios of ≥ 2 or ≤ 0.5 were chosen as cutoff values, defining increased and decreased expression, respectively. Filtered genes identified as differentially expressed by twofold or greater in both comparisons were tested for statistical significance using moderated *t* statistics by the empirical Bayes method in the R package "limma" (Smyth, 2004). For moderated *t*-test, we choose a threshold of $P < 0.05$. The corresponding false-discovery rate was 0.076, meaning that 7.6% of the genes selected by this *P* value could be false-positive (Benjamini and Hochberg, 1995).

For biological interpretation of the differentially expressed genes, the number of appearances of each gene ontology (GO) term (http://www.geneontology.org/) was counted from each list of genes. Fisher's exact test to assess the significance for enrichment of genes within three kinds of GO categories (BP, biological process; MF, molecular function; CC, cellular component) in a list was performed by the GO Browser tool in GeneSpring GX 7.3.1 (Agilent Technologies, Santa Clara, CA).

We also performed a pathway analysis with parametric analysis of gene-set enrichment (PAGE; Kim and Volsky, 2005) to analyze the differential expression of predefined gene sets rather than individual genes. This test was implemented by calculating a Z score for a given gene set that measures the deviation of the average log-ratio for genes in the category

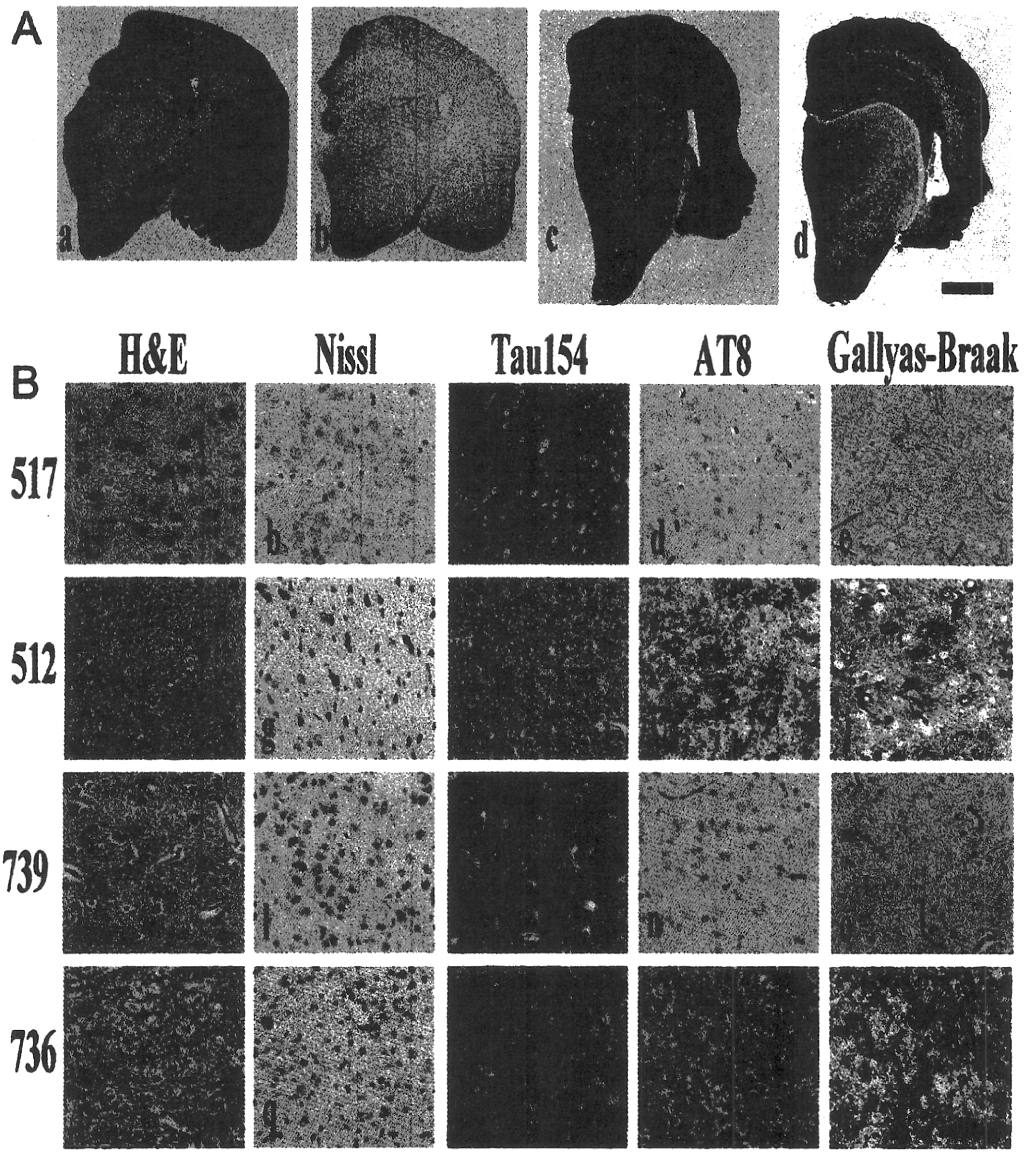

Fig. 1. Phenotypic variation in TgTauP301L mice. **A**: Brains of 739 (a,b) and 736 (c,d); a and c show tau154 staining, and b and d show Gallyas-Braak silver staining. Accumulation of human tauP301L was similar between 739 and 736. However, severe NFTs and brain atrophy were prominent in 736 (d). **B**: Brain sections of 517, 512, 739, and 736 were stained with hematoxylin and eosin (H&E; a,f,k,p), Nissl (b,g,l,q), tau154 antibody (c,h,m,r), AT8 antibody (d,i,n,s), and Gallyas-Braak silver staining (e,j,o,t). Neuronal cell losses and NFT formation were prominent in 512 (g,j) and 736 (q,t). Scale bar = 1 mm in A; 50 μm in B. [Color figure can be viewed in the online issue, which is available at wileyonlinelibrary.com.]

from the genome-wide average, in units of the standard deviation. The Z score for each category was calculated as

$$Z = (\bar{X} - \mu)\sigma/\sqrt{n},$$

where μ and σ represent the mean and the standard deviation of total -fold change values of genes after filtering by MAS5 detection call, respectively. $\bar{X}$ is the mean of -fold change values of genes for a given set, and n is the size of a given gene set. The predefined gene sets were created from GenMAPP (http://www.genmapp.org/).

Immunostaining

Tissues were fixed in 4% paraformaldehyde with 0.1 M phosphate buffer (pH 7.6) for 8 hr and embedded in paraffin. Five-micrometer-thick sections were prepared for immuno-

staining and Gallyas-Braak silver stain. For tau immunostaining, sections were immersed in 0.5% periodic acid for blocking intrinsic peroxidase and treated with 99% formic acid for 3 min. After blocking with 5% normal goat or horse serum, sections were incubated overnight with primary antibodies. The specific labeling was visualized using Vectastain Elite ABC kit (Vector, Burlingame, CA). Tissue sections were counterstained with hematoxylin. The following antibodies were used for immunostaining: tau154 (1:200), TAU-5 (1:1,000; Biosource. Camarillo, CA), AT8 (1:400; Innogenetics, Gent, Belgium; Murakami et al., 2006), antibodies to ApoD (1:1,000; Patel et al., 1995; 36C6, 1:100; Novocastra Laboratories, Newcastle, United Kingdom), antibodies to DCX (N-19, 1:200; C-18, 1:200; Santa Cruz Biotechnology, Santa Cruz, CA), antibody to Npas4 (1: 50, polyclonal antibody to purified Npas4; 1:100, NBP1-06574; Novus Biologicals, Littleton, CO), and antibody to Kcnab1 (1: 50; Santa Cruz Biotechnology).

Western Blotting

The remaining brain sample was homogenized in 9 volumes of Tris-saline buffer with protease inhibitors (Complete Inhibitor Cocktail tablets; Roche, Mannheim, Germany) and centrifuged at 55,000 rpm for 60 min at 4°C (TS buffer-soluble fraction). The pellet was homogenized again in 4 volumes of 1% sarkosyl in TS, incubated on ice for 30 min, and centrifuged at 55,000 rpm for 60 min at 4°C. The pellet was analyzed as the sarkosyl-insoluble fraction. The samples were boiled at 70°C in 4 volumes of SDS sample buffer, separated on 4–12% NuPAGE Bis-Tris Gel (Invitrogen, Carlsbad, CA), and the blots were labeled by antibodies. Signals were visualized with an enhanced chemiluminescence detection system (Pierce United Kingdom) and quantified by a luminoimage analyzer (LAS 1000-mini; Fuji Film, Tokyo, Japan). The signals were corrected by those of β-actin, and were tested for statistical significance using *t*-tests [TgTauP301L with NFTs and neuronal cell losses (n = 3) and without NFTs and neuronal cell losses (n = 3)]. All animal experiments were performed according to guidelines established in the *Guide for the care and use of laboratory animals* and by the ethical committee of Hirosaki University.

RESULTS

In comparing gene expression ratios between 517 and 512, 278 were increased and 162 were decreased. There were 477 increased gene expression ratios and 369 decreased gene expression ratios between 739 and 736. In the two comparisons of gene expression ratios, there were 52 up-regulations and 16 down-regulations in common. Among these 68 gene expressions, 37 gene expressions were significant, and 24 genes have already been described (Table I). There was no alteration of gene expression ratios for APP, MAPT, or GSK3β in 517, 512, 739, and 736 mouse brains.

According to biological pathways and gene expression groupings based on the GenMAPP database, comparison between 517 and 512 demonstrated seven down-regulated gene expression ratio groups. Five pathways consisted of up-regulated gene expression ratio groups. On comparison between 739 and 736, only one pathway showed a down-regulated gene expression group; however, 41 pathways showed up-regulated gene expression groups. Among these biological pathways, inflammatory response, mitochondrial fatty acid beta-oxidation, oxidative stress, apoptosis, and complement and coagulation cascades were commonly up-regulated.

To confirm further the differences in gene expression profile associated with NFT formation and neuronal cell losses, ApoD (Muffat and Walker, 2010), Npas4 (Lin et al., 2008), DCX (Moores et al., 2004), and Kcnab1 (Need et al., 2003) were selected for analysis at the protein level of up- or down-regulated genes among 24 significant genes because of the availability of antibodies. ApoD and DCX gene products had been previously suggested to be altered in AD (Thomas et al., 2003; Jin et al., 2004); however, others have not been reported.

On immunostaining, ApoD was markedly labeled in the brain of TgTauP301L with NFTs and neuronal cell losses compared with those of TgTauP301L without NFTs and neuronal cell losses. In particular, the hippocampus and white matter were markedly stained (Fig. 2b). Enhanced ApoD immunostaining was not detected in brains of TgTauP301L without NFTs and neuronal cell losses (Fig. 2a). The areas that exhibited extensive ApoD immunoreactivities were not related to those showing NFT formation and neuronal cell losses. Increased ApoD immunostaining was detected in neuronal processes, oligodendrocytes, and astrocytes (Fig. 2d) compared with that in 739 brains (Fig. 2c). Astrocytosis was also prominent in these areas. In AD and tauopathy brains, ApoD immunostaining was also detected mainly in astrocytes of the white matter and rarely in neurons in the cortex (Fig. 2f,g,i,j). ApoD was not detected in the control normal human brains (Fig. 2e,h).

Markedly decreased DCX immunoreactivities were observed in TgTauP301L showing NFTs and neuronal cell losses (Fig. 2l,n). Decrease in DCX-positive cells was observed even in areas without NFT formation. DCX-positive cells were detected in the dentate gyrus, hippocampus, and cerebral cortex of age-matched control nontransgenic mouse and TgTauP301L without NFTs and neuronal cell losses. Band-like immunoreactivities were prominent in the hippocampus of control age-matched nontransgenic mice (Fig. 2k,m). In AD and tauopathy brains, reticular immunoreactivity of DCX was markedly decreased in the dentate gyrus (Fig. 2p,q,s,t) compared with that in control human brains (Fig. 2o,r).

On Western blotting, the amount of DCX was decreased and the level of ApoD was increased in TgTauP301L mice with NFTs and neuronal cell losses compared with those in TgTauP301L without NFTs and neuronal cell losses (Fig. 3). The amounts of DCX and ApoD in sarkosyl-soluble fraction of the brain were correlated with the amount of sarkosyl-insoluble tau of the brain, suggesting that down-regulation of DCX and up-regulation of ApoD were closely associated with

TABLE I. Twenty-Four Up- and Down-Regulated Genes Shared in the Two Comparisons (517 vs. 512 and 739 vs. 736)

Description	Symbol	*P* value	Fold change (512/517)	Fold change (736/739)	Cell adhesion	Cell communication	Nervous system development	Development	Transport	Localization	DNA metabolism	Metabolism	Inflammatory response	Response to stimulus
Up-regulated														
Neuronal PAS domain protein 4	Npas4	0.03	2.33	2.77		*						*		
Thyrotropin releasing hormone	Trh	0.02	2.42	2.07		*								*
Immunoglobulin heavy chain 6 (heavy chain of IgM)	Igh-6	0.03	2.13	3.68		*			**	*		*		*
Syndecan 4	Sdc4	0.02	2.17	2.08										
Insulin receptor substrate 4	Irs4	0.02	2.11	2.10		*								
C-type lectin domain family 7, member a	Clec7a	0.04	2.21	6.62	**	*			**	*			**	*
Predicted gene 98	Gm98	0.02	3.50	2.90										
Holliday junction recognition protein	Hjurp	0.02	3.53	4.60										
Calcium/calmodulin-dependent protein kinase II inhibitor 1	Camk2n1	0.02	7.54	2.43										
Perilipin 4	Plin4	0.04	5.36	4.77										
Pyruvate dehydrogenase kinase, isoenzyme 4	Pdk4	0.03	2.80	2.28		*						*		
Proteasome (prosome, macropain) 26S subunit, ATPase 3, interacting protein	Psmc3ip	0.01	2.98	3.36							**	*		
Serine (or cysteine) peptidase inhibitor, clade A, member 3N	Serpina3n	0.02	2.65	5.47										*
Apolipoprotein D	Apod	0.03	2.05	3.55					**	*				
Periostin, osteoblast specific factor	Postn	0.02	2.01	2.23	**	*		*						
Carboxypeptidase M	Cpm	0.02	2.08	2.18								*		
Myelin-associated oligodendrocytic basic protein	Mobp	0.02	2.08	2.00										
Down-regulated														
Membrane protein, palmitoylated 4 (MAGUK p55 subfamily member 4)	Mpp4	0.01	0.40	0.29										
Pituitary tumor-transforming gene 1	Pttg1	0.00	0.09	0.11							**	*		*
Doublecortin	Dcx	0.01	0.39	0.32		*	**	*		*				
Potassium voltage-gated channel, shaker-related subfamily, beta member 1	Kcnab1	0.02	0.40	0.47					**	*				
RNA binding motif protein 45	Rbm45	0.00	0.27	0.26			**	*						
Succinate dehydrogenase complex, subunit A, flavoprotein (Fp)	Sdha	0.01	0.36	0.16					**	*		*		
RIKEN cDNA 4933400F03 gene	4933400 F03Rik	0.02	0.50	0.50										

*$P < 0.05$.

**$P < 0.01$.